Effective use of Thermal Potential of Solar Photovoltaic Module

AN APPROACH TO SOLAR PV-TE HYBRID SYSTEM

▪ ▪ ▪ ▪ ▪ ▪ ▪

A
PROJECT REPORT
Submitted in the fulfillment of the requirement of Degree of

Bachelor of Technology

In
Mechanical Engineering
By

UBAID UR REHMAN ¦ VISHESH KUMAR

SANTOSH VERMA ¦ SALMAN ¦ UTKARSH TYAGI

(Students of B.Tech Final Year, Batch 2016-2020)
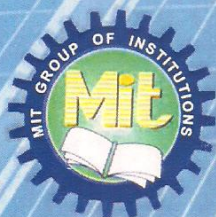
Under the Guidance of

DR. NITIN AGARWAL   DR. ABHISHEK SAXENA   MR. ARVIND KR. SINGH

Professor   Associate Professor   Assistant Professor

In Pursuit of Excellence

DEPARTMENT OF MECHANICAL ENGINEERING

MORADABAD INSTITUTE OF TECHNOLOGY

Ram Ganga Vihar, Phase-II, Moradabad-244 001 (U.P.)

Dr. Munish Chhabra
Professor & Head
Deptt. of Mechanical Engg.
Moradabad Institute of Technology
Moradabad - 244001

Acknowledgement

▪▪▪▪▪▪▪

Ubaid Ur Rehman *(Group Leader)*

Vishesh Kumar

Santosh Verma

Salman

Utkarsh Tyagi

(Students of B.tech Final Year, Batch 2016-2020)

Dr. Munish Chhat
Professor & Head
Deptt. of Mechanical Engg.
Moradabad Institute of Technology
Moradabad - 244001

Certificate

This is to certify that the Project entitled **"Effective use of Thermal Potential of Solar Photovoltaic Module – An approach to Solar PV-TE Hybrid System"** submitted by **Ubaid Ur Rehman** *(Group Leader, Roll No. 1608240085)* and other group members in partial fulfillment of the requirement of Degree of B.Tech in Mechanical Engineering, embodies the work done by them under my guidance.

Name of Group Members	Roll No.
Ubaid Ur Rehman *(Group Leader)*	1608240085
Vishesh Kumar	1608240092
Santosh Verma	1608240075
Salman	1608240074
Utkarsh Tyagi	1608240086

Project Guide : Dr. Nitin Agarwal (Professor)

Deptt. of Mechanical Engg., Moradabad Institute of Technology, Moradabad

Signature of the Guide

Date : 28·08·2020

Dr. Munish Chhabra
Professor & Head
Deptt. of Mechanical Engg.
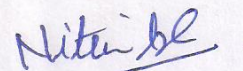Moradabad Institute of Technology
Moradabad – 244001

iii

Nomenclature

Abbreviations

PV	Photovoltaic
PVM	Photovoltaic Module
PVT	Photovoltaic Thermal
TE	Thermoelectric
TEM	Thermoelectric Module
TEG	Thermoelectric Generator
CPV	Concentrating Photovoltaic
CSP	Concentrating Solar Power
BIPV	Building-Integrated PV
IR	Infrared
UV	Ultraviolet
PCM	Phase-change Material
PCT	Phase-change Temperature
LHS	Latent Heat Storage
EVA	Ethylene-vinyl acetate
PVF	Poly-vinyl fluoride
STC	Standard test condition
AM	Air mass
FF	Fill Factor
RD	Relative Density
SMD	Surface mount device
PCB	Printed circuit board
LED	Light emitting diode
Al	Aluminum
Si	Silicon
Ge	Germanium
Pb	Lead
Bi	Bismuth
Te	Tellurium
Se	Selenium
Sb	Antimony
Cu	Copper

English Symbols

k	Thermal conductivity, W/mK
S	Seebeck coefficient, V/K
ZT_m	Modified Figure of merit
ZT	Figure of merit
Z	Figure of merit, K^{-1}
T	Temperature, K or °C
T_m	Mean Temperature, K
T_{nc}	Nominal Operating cell Temp., K or °C
P	Power, W
V	Voltage, V
I	Current, A
L	Length, m
W	Width, m
H	Height, m
A	Surface Area, m^2
t	Thickness, m
c	Specific Heat capacity, kJ/kgK
N_f	Number of Fins
N_{TE}	Number of TE Modules
s	Spacing between Fins, m
R	Resistance, Ω (ohm)
N	Number of p-n pair
G_T	Solar Irradiance, W/m^2
G_o	Actual Solar Irradiance striks on cell, W/m^2
Y	Rated capacity, W
f	Derating Factor
Q	Heat transfer rate, W
h	Heat transfer coefficient, W/m^2K
u	Speed (Velocity), m/s
E_{in}	Actual Energy input to PVM, W

Greek Symbols

σ	Electrical conductivity, $\Omega^{-1}m^{-1}$
η	Efficiency
η_m	Module Efficiency
β	Temp. coefficient of max. power, $°C^{-1}$
α	Absorptivity
ρ	Resistivity
τ	Transmissivity
ε	Emissivity
κ	Thermal conductance, W/K
σ	Stefan–Boltzmann constant, W/m^2K^4

Subscripts

max	Maximum
OC	Open-circuit
SC	Short-circuit
PV	Photovoltaic
mp	Maximum of PV module
c	Cell (PV cell)
C	Cold side
H	Hot side
STC	Standard Test Condition
g	Cover Glass
ted	Tedlar
wax	Wax
f	Fin
TE	Thermoelectric
L	Load
car	Carnot
w	Wind
sky	Sky
conv	Convection
rad	Radiation

List of Tables

Dr. Munish Chhabra
Professor & Head
Deptt. of Mechanical Engg.
Moradabad Institute of Technology
Moradabad - 244001

v

List of Figures

■■■■■■■

Dr. Munish Chhabra
Professor & Head
Deptt. of Mechanical Engg.
Moradabad Institute of Technology
Moradabad - 244001

Dr. Munish Chhabra
Professor & Head
Deptt. of Mechanical Engg.
Moradabad Institute of Technology
Moradabad - 244001

Problem Statement

An ever-increasing world population and the evolutionary development of industries combined with a large increase in energy demand has led to an important environmental crisis that already shows its clear beginning. This leads us to find sources of energy that are abundant and green. Solar energy is one such source that solves both these problems. Solar energy can be a key resource of power production for every nation because it has sufficient potential to stop the scarcity of non-renewable resources by fulfilling the demand for electricity single-handedly. Another reason is that conventional power plants emit a large amount of carbon or greenhouse gases that are harmful to our society, so, for a sustainable future a shift needs to be made towards solar energy which is eco-friendly and green energy.

Dr. Munish Chhabra
Professor & Head
Deptt. of Mechanical Engg.
Moradabad Institute of Technology
Moradabad – 244001

Objective

■ ■ ■ ■ ■ ■ ■

To develop a "Solar Photovoltaic (PV)-Thermoelectric (TE) Hybrid System" for unlocking the potential of solar energy by effective use of Thermal Potential of Solar PV module and it would be accomplished by acquiring two objectives-

1. To improve the efficiency of the solar panel by dissipating the heat with a high rate from its surface using metallic fins.
2. To utilize the excess heat of the solar panel for generating electricity by using the Thermoelectric phenomena.

Abstract

■■■■■■■

Solar energy is one of the most abundant and green source of energy among all renewable energy resources. Researchers are continually striving to improve the efficiency of the Solar Photovoltaic Module (PVM) by maintaining it below maximum allowable temperature. Accordingly, the excessive heat generated within solar PVM must be dissipated efficiently in order to avoid excessive high temperature, which has an adverse effect on the performance of the solar cell.

In this series, the main objective of the project is to improve the efficiency of solar PVM not limited by dissipating the excessive heat but also effectively utilize it by making some modifications in existing solar PVM. To achieve the objective of the project a comparison has been made between two modified PVM with a third standard one. All three Module are named such as Module-1 is the standard solar PVM, Module-2 is the solar PV-Fin Module that is a modified solar PVM with rectangular metallic fins to dissipate the excessive heat by natural convection, and Module-3 is the solar PV-TE Module another modified solar PVM with Thermoelectric Module (TEM), rectangular metallic fins, and Phase-change material (PCM) to utilize the excessive heat into further electricity. In this project, the main focus is on Module-3 that is an approach towards Solar PV-TE Hybrid System. Therefore, an experimental study is presented to analyze how much and which module between Module-2 and Module-3 will give the best performance as compared to Module-1 (standard solar PVM) which will confirm that either dissipation of excessive heat (in Module-2) or utilization of excessive heat (in Module-3) would be the best way to enhance the efficiency of solar PVM.

The experimental results show that the Module-2 (Solar PV-Fin Module) is most efficient among Module-1 and Module-3 in respect of power, temperature, and efficiency. Module-2 and Module-3 show an average reduction in temperature by 8.70% and 4.97%

Dr. Munish Chhabra
Professor & Head
Deptt. of Mechanical Engg.
Moradabad Institute of Technology
Moradabad-244001

x

respectively w.r.t Module-1, an average increment in the power output by 14.42% and 8.72% respectively w.r.t Module-1, and an average increment in the efficiency by 14.04% and 8.18% respectively w.r.t Module-1. And the utilization of excessive heat in Module-3 by TEMs was found 0.838 Watt with a maximum efficiency of 1.27%.

The overall performance of Module-3 (including TEMs) was found the same as Module-2 and slightly lower than Module-2 in case of excluding TEMs from Module-3.

Table of Content

Dr. Munish Chhabra
Professor & Head
Deptt. of Mechanical Engg.
Moradabad Institute of Technology
Moradabad - 244001

Chapter-1
Introduction

The sun emits the radiation at the rate of 3.8×10^{26} W, only a tiny fraction of approximately 1.7×10^{17} W is accepted by the earth. In a single hour, the amount of power from the sun that strikes the Earth is more than the entire world consumption in a year. Each hour, 430 quintillion joules of energy from the sun hits the Earth while on an average, the world's total energy consumption in a year is 570 quintillion (10^{18}) joules and that is increasing day by day. The question arises on how we can use this huge amount of energy that is sufficient to fulfill the requirement of the one year world's energy consumption in a single hour. So the answer is provided that the solar irradiation on the earth is 1000-500 W/m^2 (varies location to location and throughout day hours), if we are capable to collect this irradiation by covering the whole Earth's surface with such a devices that convert the solar energy (thermal energy) into useful work (electricity) then we can utilize the exergy of this whole solar irradiation. In this series currently we are using two solar technologies, one is Concentrating solar power system (CSP) and another is Solar photovoltaic system (PV). The Concentrating solar power system occupies more space as compared to the Solar photovoltaic system for the same power output, so the solar PV system is more popular for the same reason and also it converts solar energy directly into electricity unlike concentrating solar power system. Another reason is that conventional power plants emit a large amount of carbon or greenhouse gases that are harmful to our society, so, for a

Fig. 1.1 Solar PV power plant
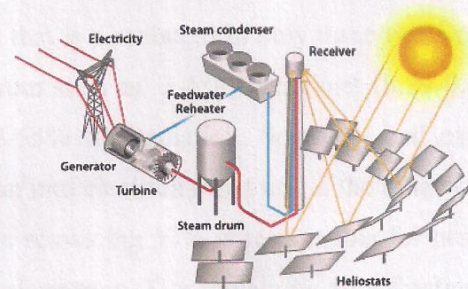
Fig. 1.2 Concentrating Solar power plant

Dr. Munish Chhabra
Professor & Head
Deptt. of Mechanical Engg.
Moradabad Institute of Technology
Moradabad-244001

14

sustainable future a shift needs to be made to solar energy, especially solar PV system which is eco-friendly and green energy. However, there are some issues with the solar PV system i.e., low efficiency because it converts only 16-20 % part of solar energy into electricity and high cost.

When the solar irradiance falls on the solar PVM (solar panel), it starts to warm up due to the generation of excessive heat within the solar PVM, and the temperature of the backsheet of the solar PVM becomes high. Due to the high-temperature difference between environment (ambient) and the backsheet of PVM, heat is rejected in the form of IR radiation (thermal energy/heat) that has the potential to produce further electricity. As it is found in the literature, the excessive heat generated within solar PVM must be dissipated efficiently in order to avoid excessive high temperature, which has an adverse effect on the performance of the solar cell. Accordingly, to sort out this problem many types of research have been and are being conducted. In addition to the series of above researches, the main objective of the project is to improve the efficiency of solar PVM not limited by dissipating the excessive heat but also effectively utilize it into further electricity by making some modifications in existing solar PVM, so there is a need of such a system that would be capable to utilizes both visible (from solar irradiation) and IR radiation (thermal energy/excessive heat of the solar panel) and would convert it into useful work (electricity). Therefore, to utilize both visible and IR radiation (excessive heat) some modification has been made in existing solar PVM (Module-3) that will be an approach to "Solar PV-TE Hybrid System", a combined technology based on both Photovoltaic effect as well as Thermoelectric effect. The Photovoltaic effect is used in solar PV that converts the visible portion of sunlight directly into electricity and the Thermoelectric effect is used in TEM that converts the IR radiation (Heat energy/Thermal energy) directly into electricity.

The spectrum of Solar radiation comes into the Earth's atmosphere consists of a range of wavelengths of radiation of 0.29-3.5 µm that is distributed in only three types of radiation out of the whole electromagnetic spectrum such as 3-5% Ultraviolet (0.29-0.4 µm), 42-43% Visible light (0.4-0.7 µm) and 52-55% IR Radiation. Solar PV cell can converts only a 47% fraction of total solar radiation into electricity that lies in the range of 0.30-1.1 µm almost falls in Visible region and the remaining 53% is responsible for heat generation in the solar PVM which degrades its performance. This remaining 53% fraction lies in almost in the IR region and has only a tiny fraction of UV radiation and both are not

able to create the electron-hole pair. Due to the shorter wavelength of UV radiation, it is absorbed by the upper surface of the solar cell before reaching the p-n junction and increases the internal energy of the cell that results in the generation of heat. Whereas in the case of IR radiation, due to large wavelengths it is completely transmitted by the solar cell and strikes on the backsheet of the solar PVM, again results in the generation of heat. This fraction of radiation that lies almost in IR radiation is responsible to degrade the performance of the solar cell.

Consequently, the combination of the photovoltaic and thermoelectric effects would enable the utilization of a wider solar spectrum. Besides, the combination of both systems can unlock the potential of solar energy that is locked in the form of Thermal potential of solar PVM as well as to increase the efficiency of solar PVM by increasing the heat transfer rate from the panel. By unlocking the locked potential of solar energy with optimization in efficiency this system becomes more advantageous than the existing solar systems. That is, the focus is not only to reduce the temperature of the solar panel but also to unlock the locked thermal potential efficiently.

The components and auxiliaries used in the project are as follows as-

1.1 Solar Photovoltaic Module (PVM)
1.2 Thermoelectric Module (TEM)
1.3 Heat sink / Metallic Fins
1.4 Thermal-Conductive Adhesive / Glue
1.5 Phase change material (PCM) / Paraffin Wax

1.1 Solar Photovoltaic Module (PVM):

Photovoltaic solar panel absorbs solar radiation (visible light) as a source of energy to generate direct electricity (high-grade energy) that accomplished by the helioelectrical process. A solar panel consists of a large number of photovoltaic cells (approx. 50-60). A solar cell, or photovoltaic cell, is an electrical device that converts the energy of light directly into electricity by the photovoltaic effect, which is a physical and chemical phenomenon.

Fig. 1.3 Silicon Monocrystalline Solar cell

Solar cell based on photovoltaic effect. Photovoltaic effect, process in which two dissimilar materials in close contact produce an electrical voltage when struck by light or other radiant energy. Light striking crystals such as silicon or germanium, in which electrons are usually not free to move from atom to atom within the crystal, provides the energy needed to free some electrons from their bound condition. Free electrons cross the junction between two dissimilar crystals more easily in one direction than in the other, giving one side of the junction a negative charge and, therefore, a negative voltage with respect to the other side, just as one electrode of a battery has a negative voltage with respect to the other. The photovoltaic effect can continue to provide voltage and current as long as light continues to fall on the two materials.

Solar cell is composed of a very thin film (wafer) of an n-type semiconductor joined with a significantly thicker layer of the p-type semiconductor. These n-type and p-type semiconductors are made up of silicon monocrystalline/polycrystalline doped with nitrogen and boron respectively. These wafers of semiconductors are sandwiched between two sets of finger type metallic strips and are used for collecting the emitted electrons and holes that are knocked out by absorbing the energy of the photons emitted on the immobile ions present in the depletion layer at the p-n junction. This whole assembly is encapsulated by applying the transparent layer of ethylene-vinyl acetate (EVA) to making it dustproof. An
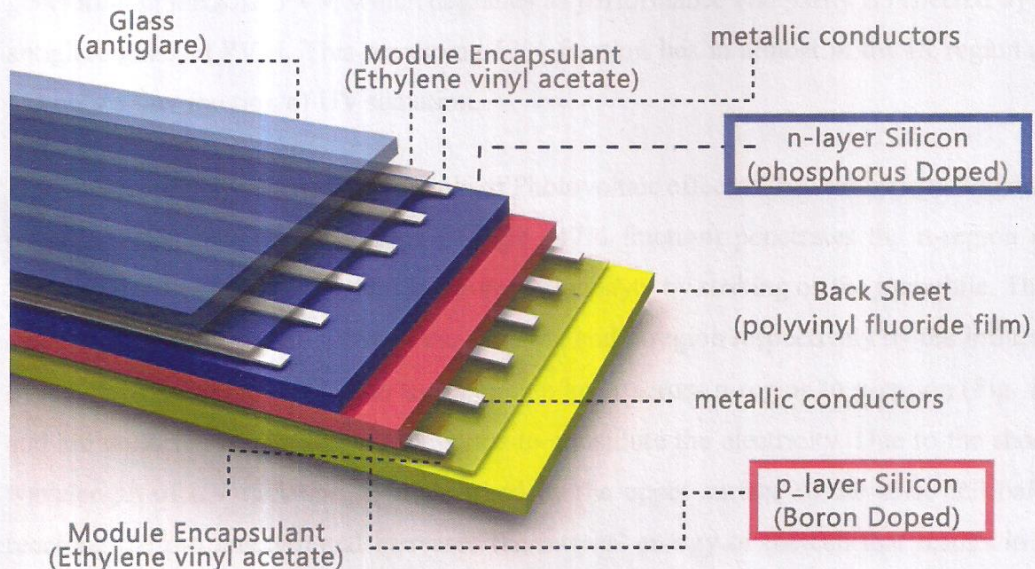
Fig. 1.4 Construction diagram of Solar cell

Dr. Munish Chhabra
Professor & Head
Deptt. of Mechanical Engg.
Moradabad Institute of Technology
Moradabad - 244001

17

antiglare glass sheet is attached on the top and a Poly-vinyl Fluoride (PVF) backsheet is on the bottom side to make it water, weather, and vibrational proof. In the last a junction is connected to the backside where the battery or load is connected (Fig. 1.4).
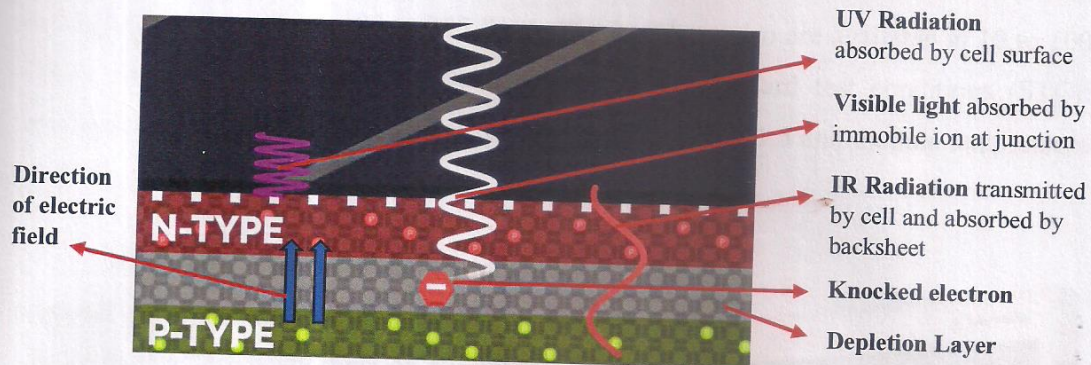
Fig. 1.5 Absorption of Visible light at P-N junction and working of Solar cell

The spectrum of Solar radiation comes into the Earth's atmosphere consists of a range of wavelengths of radiation of 0.29-3.5 μm that is distributed in only three types of radiation out of the whole electromagnetic spectrum such as 3-5% Ultraviolet (0.29-0.4 μm), 42-43% Visible light (0.4-0.7 μm) and 52-55% IR Radiation. Solar PV cell converts only a 47% fraction of total solar radiation into electricity that lies in the range of 0.30-1.1 μm almost falls in Visible region and the remaining 53% is partly responsible for the heat generation in the solar PVM which degrades its performance and partly is reflected by the antiglare glass of PVM. This remaining 53% fraction lies in almost in the IR region and has only a tiny fraction of UV radiation.

Solar cell works on the principle of Photovoltaic effect. When the radiation incident on solar cells, only visible region of light (47% fraction) penetrates the n-region and knocked out an electron-hole pair in the depletion layer by striking on the immobile. These electron-hole pairs free to move in the n-region and p-region respectively by the influence of the electric field developed in the depletion layer across n-region to p-region (Fig. 1.5) and are collected by the finger type strips to constitute the electricity. Due to the shorter wavelength of UV radiation, it is absorbed by the upper surface of the solar cell before reaching the p-n junction and increases the internal energy of the cell that results in the generation of heat. Whereas in the case of IR radiation, due to large wavelengths it is completely transmitted by the solar cell and strikes on the backsheet of the solar PVM,

Dr. Munish Chhabra
Professor & Head
Deptt of Mechanical Engg.
Moradabad Institute of Technology

again results in the generation of heat. This fraction of radiation that lies almost in IR radiation is responsible to degrade the performance of the solar cell.

Each module is rated by its DC output power under standard test conditions (STC), and typically ranges from 100 to 365 Watts (W) but these also are available in 10 to 100 Watts. Module performance is generally rated under standard test conditions (STC): irradiance of 1,000 W/m2, solar spectrum of AM (Air mass) 1.5 and module temperature at 25°C.

Electrical characteristics include nominal power (P_{max}, measured in W), open circuit voltage (V_{OC}), short circuit current (I_{SC}, measured in amperes), maximum power voltage (V_{MPP}), maximum power current (I_{MPP}), peak power, (watt-peak, Wp), and module efficiency (%).

In Fig. 1.6, a Loom Solar panel (Polycrystalline) as shown and has been used in project. It has a dimensions of 450x350x22 mm (LxWxH), max. power 20Wp, open circuit voltage 22.5 volt, short circuit current 1.11 ampere, max. voltage 19.25 volt, max. current 1.04 ampere, fill factor 80.08%, module efficiency 12.7%.
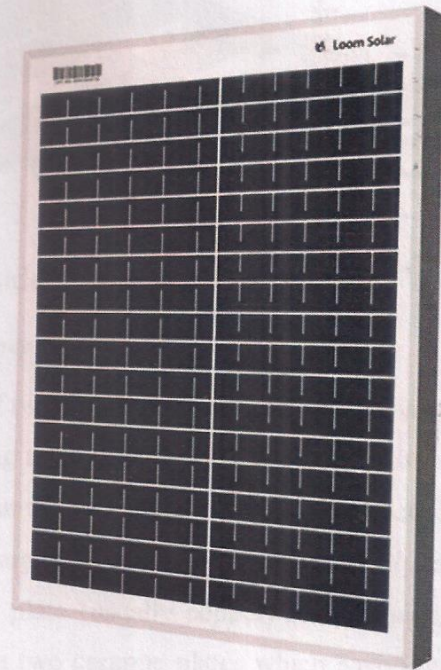
Fig. 1.6 Loom Solar polycrystalline PV module

1.2 Thermoelectric Module (TEM):
Thermoelectric module is a device that absorbs heat energy (IR radiation) as a source of energy to generate electricity (high-grade energy) directly. It is also known as a thermoelectric power generator.

It is based on the thermoelectric effect that basically consists of three effects, 1. Seeback effect, 2. Peltier effect and, 3. Thomson effect.

Here the thermoelectric module is based on Seeback effect and according to this if there is any temperature difference is found between the two junctions that made up of by connecting the two different types of materials by end to end then a potential difference is taking place between these junctions, i.e., when junctions are kept at different temperatures then the electricity produces.
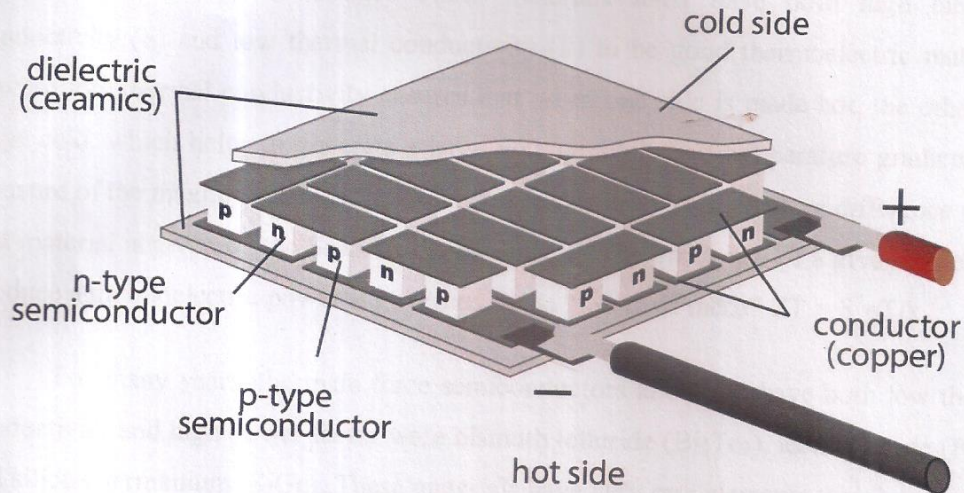
Fig. 1.7 Construction diagram of Thermoelectric module

A standard thermoelectric module consists of two unique semiconductors, one is n-type and the other one is p-type. The reason for using a different type of semiconductor is that because they have different electron densities that are necessary for the thermoelectric effect. The semiconductors are placed thermally in parallel to each other and electrically in series and then joined with a thermally conducting plate (usually copper) on each side. Finally, this whole assembly is sandwiched between two ceramic plates which have low electrical conductivity and high thermal conductivity.

When the hot side of TEM is connected to the heat source and the cold side is connected to heat sink then the majority charge carriers in both n-type (electrons) and p-type (holes) become excited by getting energy and reach to higher energy level. Now majority charge carriers (electrons and holes) start to move from the hot side to the cold side, recombine at the junction (conductive plate) and
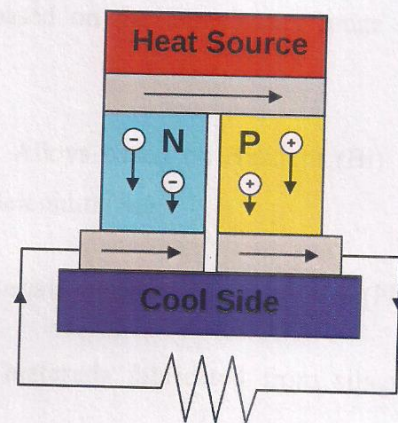
Fig. 1.8 Recombination of charge carries at P-N junction and working of TEM

finally constitute direct current (electricity). Generally, the current magnitude is directly proportional to the temperature difference.

The materials that used in TEM is known as Thermoelectric materials. Thermoelectric materials generate power directly from heat by converting temperature differences into electric voltage. These materials must have both high electrical conductivity (σ) and low thermal conductivity (k) to be good thermoelectric materials. Having low thermal conductivity ensures that when one side is made hot, the other side stays cold, which helps to generate a large voltage while in a temperature gradient. The measure of the magnitude of electrons flow in response to a temperature difference across that material is given by the Seebeck coefficient (S). The efficiency of a given material to produce a thermoelectric power is governed by its "figure of merit" $ZT = S^2\sigma T/k$.

For many years, the main three semiconductors known to have both low thermal conductivity and high power factor were bismuth telluride (Bi_2Te_3), lead telluride (PbTe), and silicon germanium (SiGe). These materials have very rare elements which make them very expensive compounds.

Today, the thermal conductivity of semiconductors can be lowered without affecting their high electrical properties using nanotechnology. This can be achieved by creating nanoscale features such as particles, wires or interfaces in bulk semiconductor materials. However, the manufacturing processes of nano-materials is still challenging.

There are many TEG materials that are employed in commercial applications today. These materials can be divided into three groups based on the temperature range of operation:

(i) Low temperature materials (up to around 450K): Alloys based on Bismuth (Bi) in combinations with Antimony (Sb), Tellurium (Te) or Selenium (Se).

(ii) Intermediate temperature (up to 850K): such as materials based on alloys of Lead (Pb)

(iii) Highest temperatures material (up to 1300K): materials fabricated from silicon germanium (SiGe) alloys.

Dr. Munish Chhabra
Professor & Head
Deptt. of Mechanical Engg.
Moradabad Institute of Technology
Moradabad - 244001

There are many advantages of TEM, some of the most crucial advantages are Eco-friendly, Solid-state construction, and small and compact but it has one main disadvantage that its efficiency very low only about 5-6%. Due low efficiency it has very large scope to modify the efficiency by developing such thermoelectric materials that have high figure of merit. Although these materials still remain the cornerstone for commercial and practical applications in thermoelectric power generation, significant advances have been made in synthesizing new materials and fabricating material structures with improved thermoelectric performance. Recent research have focused on improving the material's figure-of-merit (ZT), and hence the conversion efficiency, by reducing the lattice thermal conductivity.

Numerous types of Thermoelectric modules are available in the market and are used for different applications according to the temperature of the hot surface. Generally, the vast majority of TEMs have an ID printed on the cooled side to identify its specification and other parameters. And they are chosen based on these IDs by matching the requirement. These universal IDs indicate the size, number of stages, number of couples, and current rating in amps, as seen in the adjacent fig. 1.9.

Fig. 1.9 ID code for identification of specification and other parameters of TEMs

In fig. 1.10, a Thermoelectric Module TEC1-12706 is shown and has been used in this project. It has the dimensions 40x40x4 mm, made up of Bi_2-Te_3 semiconductors, and can be operated up to 70 °C.

Fig. 1.10 Thermoelectric Module TEC1-12706 parameters of TEMs

1.3 Heat sink / Metallic Fins:
The heat sink is a device that is used to maintain anything or components at a low temperature where cooling is a favorable condition for their proper working. It cools the component by increasing the heat transfer rate. Fins or

extended surfaces are used as a heat sink to maintain anything or components at a low temperature by increasing the heat transfer rate.

Fins transfer the heat from component to its surface by conduction mode and from its surface to the environment by convection mode, if the temperature range is very high then radiation heat transfer also takes place simultaneously with convection. Hence, heat transferred is associated with all modes of heat transfer by the fin. Generally, aluminum alloys (Al6063/Al6061) are used for the heat sink, but copper also used to meet with special requirements.
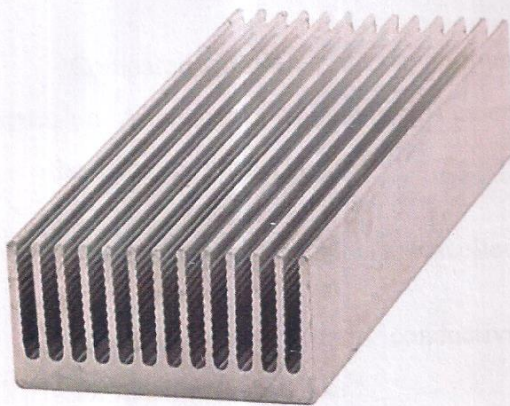
Fig. 1.11 (a) Straight Rectangular Al Fin   **Fig. 1.11 (b) Straight Pin/Cylindrical Fin**
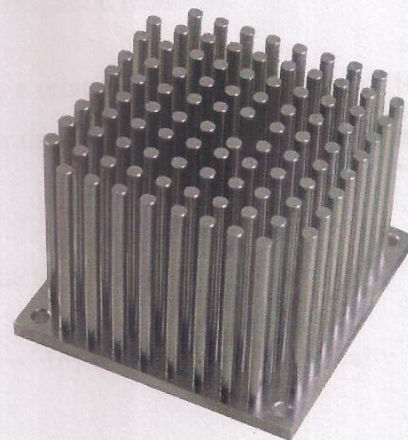
There are many types of heat fins are available in the market and are used for different applications according to load conditions (amount of heat to be removed). The most common types are straight rectangular fin and pin fin that is used for cooling of electronic components and low heat load areas (Fig. 1.11 (a) & (b)).

The use of fin (extended surface), provide efficient heat transfer. Heat transfer through fin of rectangular configuration is higher than that of other fin configurations. Temperature at the end of fin with rectangular configuration is minimum, as compare to fin with other types of configurations. The effectiveness of fin with rectangular configuration is greater than other configurations. Choosing the optimum size fin of rectangular configuration will reduce the cost for heat transfer process and also increase the rate of heat transfer. This is the reason that rectangular configuration of fin is most common. In this project straight rectangular taper fin has been used made up of Al 6063 has a thermal conductivity of ~ 167W/m-K and is typically made by extrusion (Fig. 1.11 (a)).

Dr. Munish Chhabra
Professor & Head
Deptt. of Mechanical Engg.
Moradabad Institute of Technology
Moradabad-244001

23

An Aluminum heatsink is the most widely used product for thermal solutions. Aluminum is the second most widely used metal in the world after Iron. After oxygen and silicon, aluminum is the most common element in the Earth's crust. The properties that make an aluminum heatsink popular include:

- Good thermal and electrical conductivity, Low density with a density ~ 2,700 kg/m^3
- Light weight, High strength of between 70 and 700 MPa
- Ease of malleability, Ease of machining
- Excellent corrosion resistance, Easy to recycle
- Non-magnetic which avoids interference of magnetic fields

Compared with other metals, aluminum has a relatively large coefficient of linear expansion. Aluminum's malleability is essential for the extrusion process, and in bending and other forming products.

An Aluminum heatsink is an excellent conductor of heat.

- Al 6061 has a thermal conductivity of ~ 167W/m-K and is typically used for machined heatsinks
- Al 6063 has a thermal conductivity of ~ 167W/m-K and is typically used for extruded heatsinks

Although the thermal properties are less than copper, an aluminum heatsink weighs approximately half as much as a copper conductor having the same conductivity, and is also less expensive.

Aluminum reacts with oxygen in air to form an extremely thin layer of Aluminum Oxide. Anodizing increases the thickness of the oxide layer and improves the strength of the natural corrosion protection.

1.4 Thermal-Conductive Adhesive/Glue: Thermally conductive adhesives are often used to dissipate heat from power electronics. Used to bond heat sinks, for example, their heat conductivity reduces thermal strain to prevent performance loss or failure of electronic components. Thermally conductive adhesives are also used as encapsulation compound for temperature sensors for enclosures or reactors.

There is a wide range of uses for thermally conductive adhesives within the electronics industry. The main applications include bonding SMDs (Surface Mount Devices) to PCBs (Printed Circuit Boards), bonding heatsinks for dissipating heat from circuit boards or other components, potting and encapsulating parts (including PCBs, transformers and coils). There are also applications for electric motors, batteries, lighting and LED heat transfer management.

Soldering is a quick and easy way of attaching components to PCBs. It is also very cheap and with lead-free solder now available, it has been made quite safe. However, some components parts are not suitable for soldering as they may not have "legs" which go through holes in the PCB, or they need some sort of electrical resistance to protect them and to prevent short circuits. Thermally conductive adhesives offer an ideal alternative for attaching SMDs when soldering isn't practical. They can also be used to replace mechanical assembly – offering cost and process savings and helping to reduce component weight and prevent vibration loosening and rattling.

Components, PCB and transformer coils are often "potted" inside a plastic housing (or "pot") with a potting adhesive to help dissipate heat away from the electronic part, to protect the parts against impact, vibration, environmental conditions and for security reasons.

Popular adhesive products for these applications include 1 and 2 part silicones, 2-part epoxies and polyurethanes (normally for potting). Occasionally 1-part epoxy adhesives are used, if components are not sensitive to the high temperature needed for curing the adhesive. Alternatively, special room temperature cure 1-part epoxies that do not require high temperatures for curing can be used, although these are very expensive to purchase and require special storage, shipping and handling at subzero temperatures. Other recent developments include structural acrylic adhesives which combine rapid cure speeds with strength performance and high thermal transfer rate."

On average, standard filled epoxy adhesives achieve thermal conductivity measurements of between 0.4 and 0.55 W/mK , whereas an unfilled epoxy adhesive would achieve less (which is a pity as many potting applications require a low viscosity adhesive to fill all the gaps around the components). However, specially developed thermally conductive epoxies are available with thermal conductivity of between 1.5 and 3 W/mK. It

is possible to formulate epoxies with special fillers including ceramic, metallic or nano-fillers to give this level of thermal performance. In fact, epoxy adhesives can even be blended with silver powder to give both thermal and electrical conductivity.

In Fig. 1.12, a thermal-conductive adhesive "DOWSIL SE 4420" which is one part, white color and have 4.1 MPa tensile strength, 77% elongation, 2.26 specific gravity, 48 mm fluidity, and 0.92 W/mK thermal conductivity. This "DOWSIL SE 4420 thermal-conductive adhesive has been used in this project to attach the heat fins and thermoelectric Modules.

Fig. 1.12 Thermal-Conductive Adhesive / Glue

As well as good thermal conductivity, there are other benefits commonly sought for electronics applications and for general bonding, these include;

- High strength performance – good adhesion to a wide variety of substrate materials
- Resistance to very low and very high temperatures – able to cope with differential expansion and contraction between dissimilar substrate materials (adhesive normally requires some degree of toughening)
- Resistance to chemicals, water and humidity
- Low-outgassing to minimize risk of damage to sensitive circuitry
- Non-corrosive formulation
- Resistance to thermal shock, impact and vibration
- Able to withstand solder-reflow processes
- Compliance with RoHS and REACH

1.5 Phase Change Material (PCM) / Paraffin Wax: PCM stands for

Phase Change Material. These are materials whose phase change, from solid to liquid, and liquid to solid, are used to store and release heat. In PCM's, energy is stored for use at a later time.

A phase change material (PCM) is a substance which releases/absorbs sufficient energy at phase transition to provide useful heat/cooling. Generally the transition will be from one of the first two fundamental states of matter - solid and liquid - to the other. The phase transition may also be between non-classical states of matter, such as the conformity of crystals, where the material goes from conforming to one crystalline structure to conforming to another, which may be a higher or lower energy state.

The energy released/absorbed by phase transition from solid to liquid, or vice versa, the heat of fusion is generally much higher than the sensible heat. Ice, for example, requires 333.55 J/g to melt, but then water will rise one degree further with the addition of just 4.18 J/g. Water/ice is therefore a very useful phase change material and has been used to store winter cold to cool buildings in summer since at least the time of the Achaemenid Empire.

By melting and solidifying at the phase change temperature (PCT), a PCM is capable of storing and releasing large amounts of energy compared to sensible heat storage. Heat is absorbed or released when the material changes from solid to liquid and vice versa or when the internal structure of the material changes; PCMs are accordingly referred to as latent heat storage (LHS) materials.

Latent heat storage can be achieved through changes in the State of matter from liquid→solid, solid→liquid, solid→gas and liquid→gas. However, only solid→liquid and liquid→solid phase changes are practical for PCMs. Although liquid–gas transitions have a higher heat of transformation than solid–liquid transitions, liquid→gas phase changes are impractical for thermal storage because large volumes or high pressures are required to store the materials in their gas phase. Solid–solid phase changes are typically very slow and have a relatively low heat of transformation.

There are two principal classes of phase change material: 1. organic (carbon-containing) PCMs and 2. Inorganic PCMs. But these can be classified in many categories as shown in fig. 1.13.
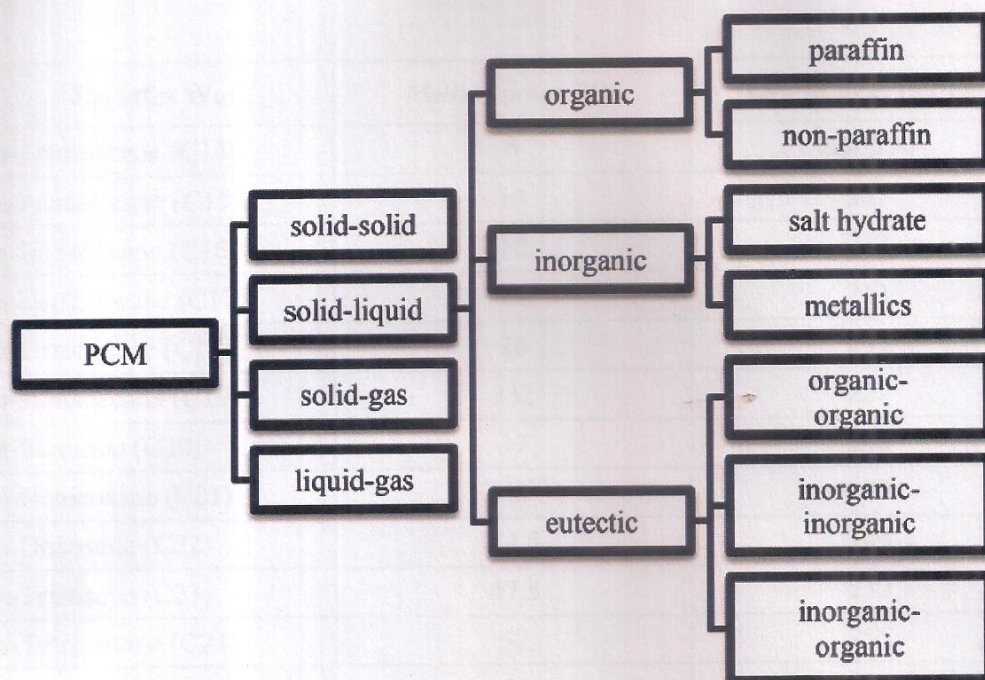
Fig. 1.13 Classification of Phase change materials (PCMs)

Paraffin wax lies in the category of organic PCM. Paraffin wax (or petroleum wax) is a soft colorless solid derived from petroleum, coal or shale oil that consists of a mixture of hydrocarbon molecules (C_nH_{2n+2}) containing between twenty and forty carbon atoms. It is solid at room temperature and begins to melt above approximately 37 °C (99 °F), and its boiling point is above 370 °C (698 °F). Common applications for paraffin wax include lubrication, electrical insulation, and candles; dyed paraffin wax can be made into crayons. It is distinct from kerosene and other petroleum products that are sometimes called paraffin.

Paraffin wax also classified on the basis of number of carbon atom present in hydrocarbons. These all paraffin waxes have different melting points, latent heat of vaporization, thermal conductivity, and density. All paraffin waxes are given below with their melting point and latent heat (Table-1.1).

In fig. 1.14, n-Heptacosane (C27) Paraffin wax is shown and has been used in this project. It has melting point 59°C, and latent heat 236 kJ/kg.

Fig. 1.14 n-Heptacosane (C27) Paraffin wax

Dr. Munish Chhabra
Professor & Head
Deptt. of Mechanical Engg.
Moradabad Institute of Technology
Moradabad - 244001

Paraffin Wax	Melting point (°C)	Latent heat (kJ/kg)
n-Tetradecane (C14)	6	228-230
n-Pentadecane (C15)	10	205
n-Hexadecane (C16)	18	237
n-Heptadecane (C17)	22	213
n-Octadecane (C18)	28	245
n-Nonadecane (C19)	332	222
n-Eicosane (C20)	37	246
n-Henicosane (C21)	40	200
n-Docosane (C22)	44.5	249
n-Tricosane (C23)	47.5	232
n-Tetracosane (C24)	52	255
n-Pentacosane (C25)	54	238
n-Hexacosane (C26)	56.5	256
n-Heptacosane (C27)	59	236
n-Octacosane (C28)	64.5	253
n-Nonacosane (C29)	65	240
n-Triacontane (C30)	66	251
n-Hentriacontane (C31)	67	242
n-Dotriacontane (C32)	69	170
n-Triatriacontane (C33)	71	268
Paraffin C16-C18	20-22	152
Paraffin C13-C24	22-24	189
RT 35 HC	35	240
Paraffin C16-C28	42-44	189
Paraffin C20-C33	48-50	189
Paraffin C22-C45	58-60	189
Paraffin C21-C50	66-68	189
RT 70 HC	69-71	260
Paraffin natural wax 811	82-86	85
Paraffin natural wax 106	101-108	80

Table-1.1 Different Types of Paraffin wax with their melting point and latent heat

Chapter-2
Literature Review

E. Radziemska (2003) presented the influence of temperature and wavelength on electrical parameters of crystalline silicon solar cell and a solar module. At the experimental stand a thick copper plate protected the solar cell from overheating, the plate working as a radiation heat sink, or also as the cell temperature stabilizer during heating it up to 80°C. A decrease of the output power (−0.65%/K), of the fill-factor (−0.2%/K) and of the conversion efficiency (−0.08%/K) of the PV module with the temperature increase has been observed. The spectral characteristic of the open-circuit voltage of the single-crystalline silicon solar cell is also presented. It is shown that the radiation-rate coefficient of the short-circuit current-limit of the solar cell at 28°C is 1.2%/(mW/cm2).

Erdem Cuce et al. (2011) carried out an experimental research concerning the effects of passive cooling on performance parameters of silicon solar cells was presented. An aluminum heat sink was used in order to dissipate waste heat from a photovoltaic (PV) cell. Dimensions of the heat sink were determined considering the results of a steady-state heat transfer analysis. The experiments were carried out for different ambient temperatures and various illumination intensities up to 1 sun under solar simulator. Experimental results indicate that energy, exergy and power conversion efficiency of the PV cell considerably increase with the proposed cooling technique. An increase of 20% in power output of the PV cell is achieved at 800 W/m2 radiation condition. Maximum level of cooling is observed for the intensity level of 600 W/m2. Performance of PV cells both with and without fins increases with decreasing ambient temperature.

Swapnil Dubey et al. (2013) studied that the operating temperature plays a central role in the photovoltaic conversion process. Both the electrical efficiency and, hence, the power output of a PV module depend linearly on the operating temperature decreasing with cell temperature. The numerous correlations for cell temperature which have appeared in the literature apply to freely mounted PV arrays, to PV/thermal collectors, and to building-

integrated photovoltaic (BIPV) installations, respectively. They involve basic environmental variables, while the numerical parameters are not only material dependent but also system dependent. Thus, one must be careful in applying a particular expression for the operating temperature of a PV module because the available equations have been developed with a specific mounting geometry or building integration level in mind. Therefore, the reader is urged to consult the original sources when seeking a correlation suitable for a particular application.

Dengfeng Du (2013) suggested that the strong solar radiation and high ambient temperature can induce an elevated Photovoltaic (PV) cell operating temperature, which is normally negative for its life span and power output. Different temperature dependences for PV performance have been reported and it has been found that the efficiency of crystalline silicon cells drops at a rate of around 0.45%/°C. Various cooling methods have been proposed to achieve lower PV cell temperature in favour of higher cell efficiencies. Passive cooling by heat spreader or heat sink can provide enough cooling to get a relatively low cell temperature even for Concentrator PV (CPV), but the heat sink surface area can be extremely large. Phase change material (PCM) system due to a choice of melting temperature, amount of material to be used, and different system designs is a promising thermal management of flat plate PV and can maintain PV temperature below its melting temperature e.g. 27 °C for a relatively long time. A facility to re-utilize of the heat energy stored in PCM is encouraged.

Adham Makki et al. (2015) studied that Photovoltaic (PV) cells can absorb up to 80% of the incident solar radiation available in the solar spectrum, however, only a certain percentage of the absorbed incident energy is converted into electricity depending on the conversion efficiency of the PV cell technology. The remainder of the energy is dissipated as heat accumulating on the surface of the cells causing elevated temperatures. Temperature rise of PV cells is considered as one of the most critical issues influencing their performance, causing serious degradation and shortening the life-time of the cells. Hence cooling of PV modules during operation is essential and must be an integral part of PV systems particularly in sun-drenched locations. Many researches have been conducted investigating a range of methods that can be employed to provide thermal management for PV systems. Among these designs, systems utilizing air, liquid, heat pipes, phase change materials (PCMs), and thermoelectric (TE) devices to aid cooling of PV cells.

Peter Atkin, Mohammed M. Farid (2015) investigated that whether the use of phase change material (PCM) infused graphite with an external finned heat sink is viable as a method of PV thermal regulation. The effect four different thermal regulation techniques (cases A, B, C and D) on the thermal performance, point-based efficiency and overall efficiency of a PV panel have been studied. These four cases are case A, the PV panel with no thermal regulation, case B, the PV panel with 30 mm thick PCM infused graphite attached to the rear, case C, the PV with a finned heat sink attached to the rear and case D, the PV panel with a combination of PCM infused graphite and finned heat sink. The results shows that out of the four thermal regulation techniques, case D was the most effective at increasing overall efficiency of the PV panel, with the greatest overall efficiency increase of 12.97. The thermal regulation effects of PCM and heat sinks are additive since the PCM creates a shift in temperature rise, whilst heat sink reduces the peak temperature. The increase in thermal conductivity of the PCM from $0.25 \text{ W m}^{-1} \text{ K}^{-1}$ to $16.6 \text{ W m}^{-1} \text{ K}^{-1}$ provided by the infusion of PCM into graphite has significant added benefits over pure PCM. Further analysis based on overall efficiency demonstrates that combining PCM with heat sinks is in fact essential.

Cătălin George Popovici et al. (2016) found that the operating temperature of photovoltaic panels represents an important parameter that influences their conversion efficiency. High operating temperatures determine a decrease of maximum output power in the same conditions of solar radiation. The study presents a numerical approach of the reduction of temperature of the photovoltaic panels by using the air cooled heat sinks. The heat sink is conceived as a ribbed wall, realized of a high thermal conductivity material. The cooling efficiency is studied for different configurations of the heat sink, obtained by modifying the angle between the ribs and the base plate. For the studied case, the operating temperature of PV panel reaches about 56 °C, if no ribs are used and the maximum produced power is 86% of the nominal one. In case of using a heat sink, even for small heights of the ribs, the average temperature of the PV panel is decreasing. On the basis of configuration of ribs, the raise of maximum power produced by photovoltaic panel is from 6.97% to 7.55% comparing to the base case, for angles of the ribs from 90° to 45° respectively.

Ahmad El Mays et al. (2017) investigated that the excess in heat must be dissipated efficiently in order to avoid excessive high temperature, which have an adverse effect on the electrical performance of the cell. Therefore, an experimental study is presented to

enhance the performance of PV panels using Aluminum finned plate, and cooling under natural convection. The use of heat sinks has been conducted to address this problem by using an optimum design of Aluminum finned plate. The results show that the use of an Aluminum finned plate has increased the solar to electrical conversion efficiency by 1.75%, and the output power by 1.86 Watt.

Linus Idoko et al. (2018) investigated that the efficiency and power output of a PV module decrease at the peak of sunlight due to energy loss as heat energy and this reduces the module power output. Multi-concept cooling technique, a concept that involves three types of passive cooling, namely conductive cooling, air passive cooling and water passive cooling has the potential to tackle this challenge. The experiment was set up using two solar panels of 250 watts each with both modules mounted at a height of 37 cm to create room for air-cooling, with the application of water-cooling at the surface of one of the PV modules to reduce the surface temperature to 20 °C. The rear of the same module attached to an aluminum, Al heat sink. The other module also mounted was without water-cooling and Al heat sink attachment. The Al heat sink comprises aluminum plate attached with aluminum fins to aid cooling, and water at a reduced temperature achieved with the introduction blocks of ice facilitated the module surface cooling. The experiment recorded an appreciable increase in the module output power with module + Al hint sink & water-cooling of the module surface temperature to 20°C, an output power increase of 20.96 W at 12:45 pm at 80% derating factor used in order to account for losses. This increase in output exceeds 250 Watts with 0% losses, and an increase in efficiency above 3%, hence the PV module and the power output were enhanced using the multi-concept cooling technique.

K. P. Amber et al. (2020) studied that at higher ambient temperatures during summer months, the cell temperature of a photovoltaic (PV) module increases to 50–60 °C and sometimes could go as high as 80 °C due to which the PV module heats up and fails to deliver its optimum output. He carried out an experimental study that focused on enhancing the efficiency of mono-crystalline photovoltaic (PV) modules by reducing their back-surface temperature. For this purpose, the heat transfer area has been increased by introducing fins at the back surface of the PV modules with two different configurations, i.e. rectangular and circular. Thermal analysis included measuring hourly module temperature, calculation of hourly Nusselt number, coefficient of convection heat transfer, and convection heat loss from the back surface of each module, whereas in terms of

33

analyzing the module's electrical performance, hourly readings were taken for the module's maximum power and efficiencies. The results showed that there was a significant effect of fins on the back surface of the PV modules. PV modules, particularly with rectangular fins having larger cross-sectional and surface area dissipated 155% more heat and generated 10.8% and 4% more power than the reference module and the circular fins-based module, respectively, and resulted in a 10.6% decrement in module temperature and an increase in module efficiency by 14.5%. The circular fins-based module dissipated only 27% more heat than the reference module. Therefore, the PV module with rectangular fins is recommended for the enhanced performance of PV installations.

Karim Egab et al. (2020) found that the temperature of a solar panel is an important parameter, which influences its performance and efficiency. Thus, development of solar panel cooling systems represents a new face of technology that may be used to improve power generation. Here, the reduction of solar panel temperature using an air-cooled heat sinks is studied numerically. The design of the heat sink comprises rectangular fins and rectangular fins with holes, made from a material with high thermal conductivity. The cooling efficiency is studied for different configurations of the heat sink, which are obtained by changing the fin numbers and hole distances. In this work, the cooling of a solar panel using air-cooled heat sinks with different configurations of fins and holes was studied numerically. The air heat sink contributed to a dramatic reduction in the panel's temperature. Furthermore, there was improvement in cooling of the heat sink obtained by changing the fin numbers and hole distances on the fins. The panel's temperature decreased with a decrease in the ambient temperature and the heat flux. Use of the fins and holes reduced the panel temperature, which improved the panel performance. Increasing the number of fins and holes decreases the panel temperature. The reduction of panel temperature with fins is 50% compared to solar panels without fins.

Parkunam N et al. (2020) studied that the photovoltaic (PV) solar cell generates electricity by receiving solar irradiance in the forms of photons. When the heat induced in the panel exceeds the operating temperature, there is drop in electrical efficiency. The objective of this project is to design the system to increase the electrical efficiency of solar cell by cooling the cell with the help of various heat sinks and wick structure with copper and aluminum fins. The heat removed from the back surface of the panel with the help of fins that absorb heat generated by the cells during the day. Therefore, the decreased temperature of PV panel increases the electrical efficiency of solar cell. When the solar

cells receive more solar radiations, it generates more electricity. At the same time, the efficiency drops when the temperature of solar cell increases. It can be concluded that the efficiency and electrical characteristics of the copper fins are higher than the aluminum by 4% and 6%, respectively.

Guiqiang Li et al. (2017) carried out an experiment and found that the electrical efficiency can be increased by combining photovoltaic (PV) and the thermoelectric (TE) systems. However, a simple and cursory combination is unsuitable because the negative impact of temperature on PV may be greater than its positive impact on TE. This study analyzed the primary constraint conditions based on the hybrid system model consisting of a PV and a TE generator (TEG), which includes TE material with temperature-dependent properties. The influences of the geometric size, solar irradiation and cold side temperature on the hybrid system performance is discussed based on the simulation. Furthermore, the effective range of parameters is demonstrated using the image area method, and the change trend of the area with different parameters illustrates the constraint conditions of an efficient PV-TE hybrid system. These results provide a benchmark for efficient PV-TEG design.

S. Mahmoudinezhad et al. (2018) investigated the transient response of a hybrid system composed of concentrated photovoltaic (CPV) cell and thermoelectric generator (TEG). He carried out by using a numerical simulation approach thermally coupled between the CPV and TEG. A transient model is established and solved by finite volume algorithm. In spite of temperatures profile in the hybrid CPV-TEG module, as results of variation of solar irradiation, power generation and efficiency of the CPV and TEG under the transient condition are presented. The results show that efficiency of the TEG and CPV varies diversely versus changing the solar radiation and module temperature. Moreover, the thermal response of the TEG stabilizes temperature fluctuation of the hybrid module when the solar radiation rapidly changes. In this work, impact of the thermal contact resistance on the temperature profile and system efficiency is investigated. The model presented in this study provides a fundamental understanding of the thermal and electrical effect of the TEG in hybrid CPV-TEG module under transient conditions.

R. Bjørk, K. K. Nielsen (2018) investigated the maximum efficiency for photovoltaic (PV) and thermoelectric generator (TEG) systems without concentration. Both a combined system where the TEG is mounted directly on the back of the PV and a tandem

system where the incoming sunlight is split, and the short wavelength radiation is sent to the PV and the long wavelength to the TEG, are considered. An analytical model based on the Shockley-Queisser efficiency limit for PVs and the TEG figure of merit parameter zT is presented. It is shown that for non-concentrated sunlight, even if the TEG operates at the Carnot efficiency and the PV performance is assumed independent of temperature, the maximum increase in efficiency is 4.5 percentage points (pp.) for the combined case and 1.8 pp. for the tandem case compared to a stand-alone PV. For a more realistic case with a temperature dependent PV and a realistic TEG, the gain in performance is much lower. For the combined PV and TEG system it is shown that a minimum ZT value is needed in order for the system to be more efficient than a stand-alone PV system.

Jin Zhang, Yimin Xuan (2019) introduced the concept of the integrated design to improve the PV-TE system. The photovoltaic-thermoelectric hybrid system (PV-TE) has attracted much attention due to its ability of utilizing solar energy in full spectra. To enhance the heat transfer, the ceramic plates of the commercial TE modules are eliminated from the PV-TE system in order to reduce the thermal resistance. To enhance the absorption of the solar energy, a V-type groove which can keep each PV cell perpendicular to its adjacent PV cells is used in the PV-TE system. An experimental setup is established to demonstrate the feasibility of the structural improvement. The results indicate that the simplified TE structure can lead to an increase in both PV efficiency and TE efficiency by enhancing the heat transfer. An obvious increase in the PV-TE efficiency caused by the V-type groove is observed in the experiment.

Samson Shittu et al. (2019) presented the concepts of photovoltaics and thermoelectric energy conversion, research focus areas in the hybrid systems, applications of such systems, discussion of the most recent research accomplishments and recommendations for future research. Effective thermal management of photovoltaic cells is essential for improving its conversion efficiency and increasing its life span. Solar cell temperature and efficiency have an inverse relationship therefore, cooling of solar cells is a critical research objective which numerous researchers have paid attention to. Among the widely adopted thermal management techniques is the use of thermoelectric generators to enhance the performance of photovoltaics. Photovoltaic cells can convert the ultra-violent and visible regions of the solar spectrum into electrical energy directly while thermoelectric modules utilize the infrared region to generate electrical energy. Consequently, the combination of photovoltaic and thermoelectric generators would enable the utilization of

a wider solar spectrum. In addition, the combination of both systems has the potential to provide enhanced performance due to the compensating effects of both systems. The waste heat produced from the photovoltaic can be used by the thermoelectric generator to produce additional energy thereby increasing the overall power output and efficiency of the hybrid system. However, the integration of both systems is complex because of their opposing characteristics thus, effective coupling of both systems is essential.

BirolKılkış (2020) developed an integrated, multi-layered, composite photovoltaic thermal (PVT) module consisting of a multitude of stand-alone mini PVT cartridges and tested a prototype. Individual PVT cartridges consist of several sandwiched layers with photovoltaic cells, TEG units, packed-bed PCM layer for thermal storage, and thermally controlled heat pipes with dynamic control. When cartridges are installed, the composite PVT module is completed by adding a flat-plate collector layer on the top. An internal array of pulse-control heat pipes maintains the total exergy output (power and heat) at a maximum by adjusting the heat flux. In such a configuration, it represents the solar equivalent of a conventional cogeneration system with a bottoming cycle. This paper summarizes the technological evolution of the new composite PVT system and provides examples of its use. Pilot-scale tests have shown that the Rational Exergy Management Model efficiency is about 25% more than a conventional PVT system and the total net electrical power output per unit solar insolation area is more than 30%. Total exergy output (power and heat) is twice as much as a conventional PVT unit in a typical summer month. The results obtained are discussed with further evolutionary recommendations. The importance of exergy-levelized unit panel cost is put forth to provide a basis for the fundamental procedure for a dedicated, well-accepted, and stand-alone PVT test method for the rating of system performance.

S. Mahmoudinezhad et al. (2019) presented an experimental investigation and numerical verification of the transient behavior of a hybrid concentrating triple junction solar cell-thermoelectric generator system. The experimental work is accomplished under varying concentrated solar radiations using a solar simulator, and the numerical study is conducted using COMSOL Multiphysics Modeling Software. An arbitrary pattern for the solar radiation varying between 0 and 39 suns is considered in the experiments and numerical simulation. Time-dependent temperatures of the concentrating triple-junction solar cell and hot and cold sides of the thermoelectric generator along with short circuit current, open circuit voltage and maximum powers are obtained experimentally. The results

indicate that the output power by the concentrating triple-junction solar cell is fluctuating very fast with changing the solar radiation. Due to the thermal capacity and thermal resistance of the thermoelectric generator, this variation for the temperatures and output power of the thermoelectric generator is more gradually. The results also indicate that using thermoelectric generator in the hybrid system leads to having more stable overall output power. Furthermore, the contribution of the thermoelectric generator in the overall power generation by the system can be enhanced with material and geometrical optimization.

P. Bamroongkhan et al (2019) devised a solar parabolic dish photovoltaic (PV)-thermoelectric (TE) power generation system and measured its behavior continuously under realistic outdoor circumstances. The effect of focal distance was also analyzed. The experimental results showed that the conversion of TE, PV and overall efficiency were 2.96, 16.69 and 19.65%, respectively at the focal distance of 57 cm. The unit obtained its electrical power out from a 2.94 W TE generator and a 1.93 W PV module. The PV module was used to drive a fan for cooling the TE generator and itself. Because of its noiseless operation, light weight, high reliability, and overall environmental friendliness, this concept can be used to solve power supply limitation for low-power wireless sensors.

A. Lekbir et al. (2019) studied the solar energy application in a large spectrum has the potential for high-efficiency energy conversion. Though, solar cells can only absorb photon energy of the solar spectrum near their band-gap energy, and the remaining energy will be converted into thermal energy. The use of the thermoelectric generator becomes a necessity for convert this thermal energy dissipated so as to increase efficiency conversion. This paper analyses the feasibility of photovoltaic-thermoelectric hybrid system and reviews their performance in order to optimize harvested energy. This method combines thermoelectric generators and the effects of heat sensitive materials associated to photovoltaic cells in phase change for generating both energy day and night. Experimental measures have been conducted primarily in laboratory conditions for a greater understanding of hybridization phenomena under real conditions and to test the actual performance of devices made. Results show that the hybrid system can generate more power than the simple PV and TEG in environmental conditions. This hybrid technology will highlight the use of renewable energies in the service of the energy production.

Chapter-3
Methodology

∎∎∎∎∎∎∎

3.1 Design and Fabrication:

Whole experimentation is carried out on the analysis of two modified solar PVM with third standard one. All three Module are named such as Module-1 is the standard solar PVM, Module-2 is the solar PV-Fin Module that is a modified solar PVM with rectangular metallic fins to dissipate the excessive heat by natural convection, and Module-3 is the solar PV-TE Module another modified solar PVM with Thermoelectric Module (TEM), rectangular metallic fins, and Phase-change material (PCM) to utilize the excessive heat into further electricity.

One by one the design and fabrication of all three modules have been discussed in details with their specification as follows-

3.1.1 Module-1: Module-1 is a standard polycrystalline Loom solar PVM of 20W maximum power (Fig. 3.1). There is no modification is done and used only to compare
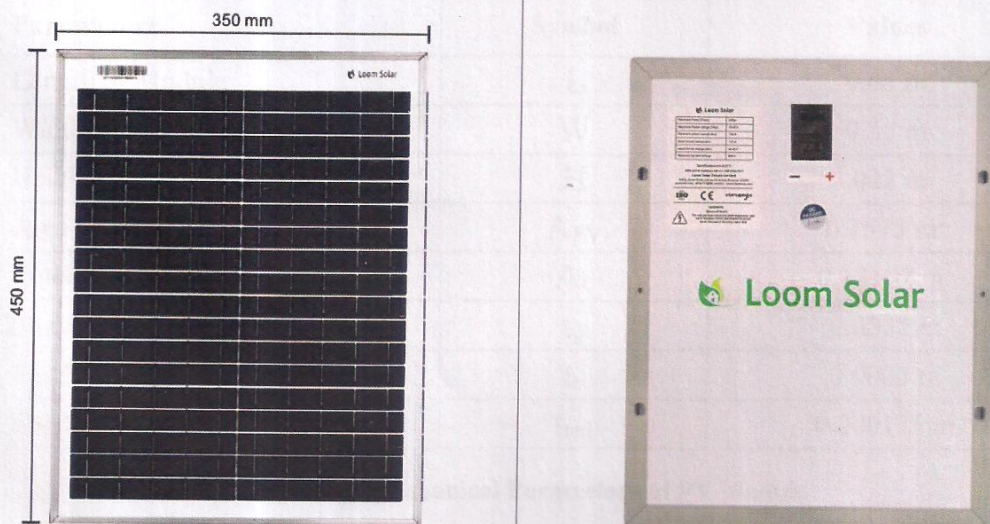

Fig. 3.1 Module-1 Standard Loom Solar PVM front and back side

the power and efficiency of two modified PVM i.e., Module-2 and Module-3.

Other parameters and specification of Loom solar PV module are given below in Table-3.1, Table-3.2 and Table-3.3

Electrical Parameters

Parameters	Symbol	Values
Maximum Power	P_{max}	20 W, ±3.0%
Open-circuit Voltage	V_{OC}	22.5 V
Short-circuit Current	I_{SC}	1.11 A
Maximum Voltage	V_{mp}	19.25 V
Maximum Current	I_{mp}	1.04 A
Fill Factor	FF	80.08 %
Module Efficiency	η_m	12.7 %
Cell Efficiency	η_c	15.2 %
Nominal Operating cell Temp.	T_{nc}	44 °C
Temp. Coefficient of Max. Power	β	-0.43 %/°C
Electrical values measured at STC: 25°C, 1.5AM, 1000 W/m²		

Table-3.1 Electrical Parameters of PV Module

Mechanical Parameters

Parameters	Symbol	Values
Length of Module	L	0.45 m
Width of Module	W	0.35 m
Height of Module	H	.022 m
Area of Module	A_{PV}	0.1575 m²
Total Area of Cells	A_c	0.13167 m²
Thickness of Cover Glass	t_g	0.0032 m
Thickness of PV cell	t_c	0.0003 m
Thickness of Tedlar (Backsheet)	t_{ted}	0.000175 m

Table-3.2 Mechanical Parameters of PV Module

Thermal Parameters

Parameters	Symbol	Values
Absorptivity of Cover Glass	α_g	0.05
Absorptivity of PV Cell	α_c	0.85
Absorptivity of Tedlar	α_{ted}	0.5
Reflectivity of Cover Glass	ρ_g	0.05
Reflectivity of PV Cell	ρ_c	0.15
Transmissivity of Cover Glass	τ_g	0.9
Emissivity of PV Cell	ε_c	0.88
Thermal Conductivity of PV Cell	k_c	148 W/mK
Thermal Conductivity of Tedlar	k_{ted}	0.2 W/mK

Table-3.3 Thermal Parameters of PV Module

3.1.2 Module-2: Module-2 is a solar PV-Fin Module which has been made by taking some modification in solar PVM with applying Aluminum Fins on the backside of PVM. Aluminum Fins increase the heat transfer rate that facilitates for removing the excessive heat by natural convection that generated during the operation of PVM due to IR radiations.

When the heat starts to flow from the backsheet (Tedlar) to ambient air, Al-Fins provide the high conductive path between the backsheet and ambient air that results in the rapid flow of excessive heat of PVM and turns reducing the temperature of PVM. And on cooling of PV module result in better performance.

Al-Fins transfer the heat from the backsheet of PVM by conduction mode and from its surface to the environment by convection mode (natural convention). Therefore, for effective cooling of PVM, optimum designing of fins is required. Effectiveness of straight

Fig. 3.2 Aluminum alloy Al-6063 Heat Fin

rectangular taper fin is more than the others section i.e., straight cylindrical fin, so straight rectangular taper the fin with proper dimensions is an optimum section for fins.

In Module-2, straight rectangular taper fin made up of aluminum alloy Al 6063 by extrusion process has been used with proper dimensions (Fig. 3.2).

Dimensions and others parameter of Al-fins are given below in Table-3.4

Parameters	Symbol	Values
Thermal Conductivity	k_f	167 W/mK
Sp. Gravity (Relative Density)	RD_f	2.7
Specific Heat Capacity	c_f	0.9 kJ/kgK
Length of Fin	L_f	0.044 m
Width of Fin	W_f	0.3 m
Thickness of Fin at Root	t_1	0.004 m
Thickness of Fin at End	t_2	0.002 m
Spacing between Fins	s	0.01 m
Number of Fins	N_f	34

Table-3.4 Dimensions and other Parameters of Al-6063 Heat Fins

Fins have been attached to the PVM with the help of thermal-conductive glue to make proper contact between PVM and Fins by removing air gaps that reduce the conduction of heat.

Thermal-conductive glue provides a good bond without any mechanical support and fills the space where the air is entrapped and increases the thermal resistance

"DOWSIL SE 4420" thermal-conductive adhesive (Fig.1.12)bhas been used to attach the heat fins. It is one part white color glue that having 4.1 MPa tensile strength, 77% elongation, 2.26 specific gravity, 48 mm fluidity, and 0.92 W/mK thermal conductivity.

3D model of Module-2 as shown in fig. 3.4 and Graphical and actual picture of Module-2 (Solar PV-Fin Module) as shown below in fig. 3.3 and

Dr. Munish Chhabra
Professor & Head
Deptt. of Mechanical Engg.
Moradabad Institute of Technology
Moradabad - 244001
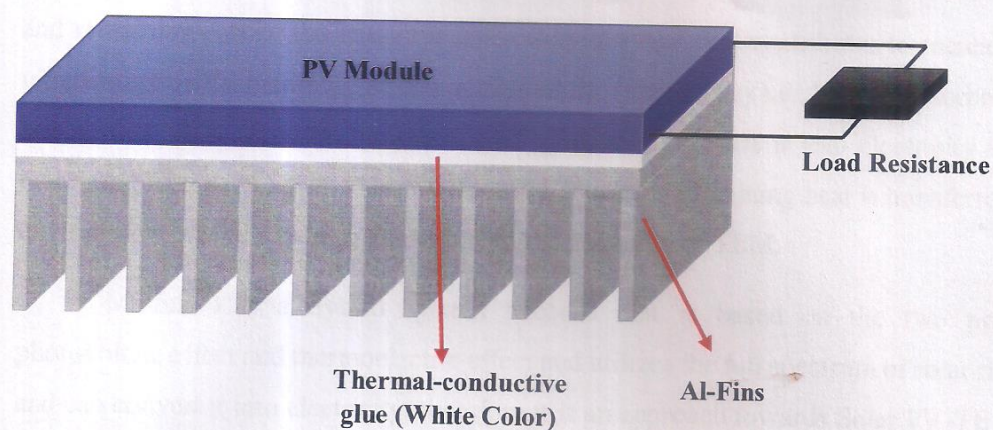
Fig. 3.3 3-D Model of Module-2 (Solar PV-Fin Module)
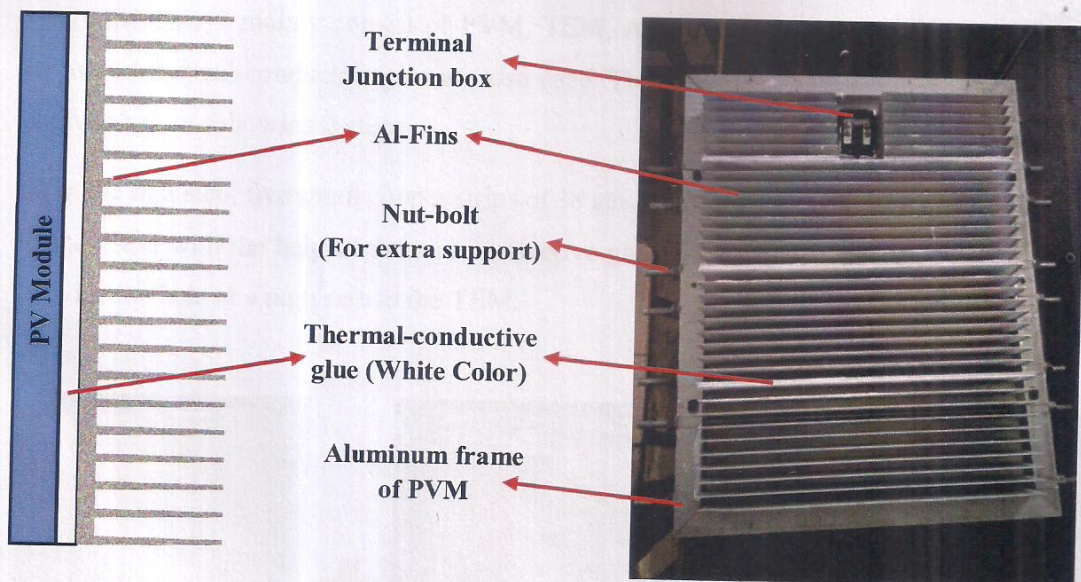
Fig. 3.4 Graphical and Actual Module-2 (Solar PV-Fin Module)

3.1.3 Module-3: Module-3 is the solar PV-TE Module which is another modified solar PVM with Thermoelectric Module (TEM), rectangular metallic fins, and Phase-change material (PCM). The purpose of this module is to convert excessive heat into electricity with the help of TEM instead of wasting it.

When the solar radiation incident on PV module, approximately 85% part is absorbed by module and only a 15% portion of this absorb part of solar energy is converted to PV electricity, another portion is lost to the environment by radiation and convection,

and remaining part of the energy is converted into heat that contributes to increasing the temperature of PV module. The last portion of the solar energy i.e., heat, is absorbed by the hot side of TEM from the backsheet of PV module converts it into electricity with the principle of Seeback Effect (Thermoelectric Effect) and remaining heat is transferred to the environment with the help of Al-fins from the cold side of TEM.

Module-3 is a hybrid system because that is based on the two principles photovoltaic effect and thermoelectric effect and utilizes the full spectrum of solar radiation and can convert it into electricity, therefore it is an approach towards Solar PV-TE Hybrid System. Photovoltaic effect works on the Visible light while Thermoelectric effect works on the IR radiation of solar radiations. There is a possibility to the utilization of Visible and IR radiation is possible in Solar PV-TE Hybrid System

Module-3 mainly consist of PVM, TEM, Al-fins, and PCM. Besides this copper strips and thermal-conductive glue are also used. The design and fabrications of Module-3 is given below following 3 steps-

(i) In the first step, five small copper strips of 38 gauge (0.1 mm thickness) have been stuck to the PVM with the help of thermal-conductive glue (Fig. 3.5). This copper strips aid to provide the heat at a high rate to the TEM.
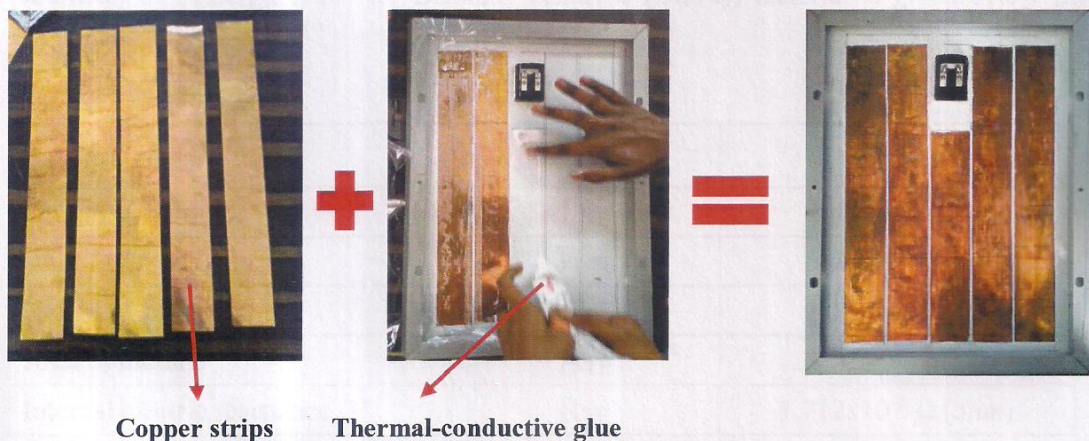

Copper strips   **Thermal-conductive glue**

Fig. 3.5 Stepwise attachment of copper strips on PVM

(ii) In the second step, thermoelectric Modules have been attached to the copper strips with the help of thermal-conductive glue. A total of 33 modules are attached to the copper strips, in which five modules have been attached to the middle strip and seven-seven modules to the 4 strips beside of middle strip (Fig. 3.6).

Thermal-conductive glue stuck on TEM   **TEM**
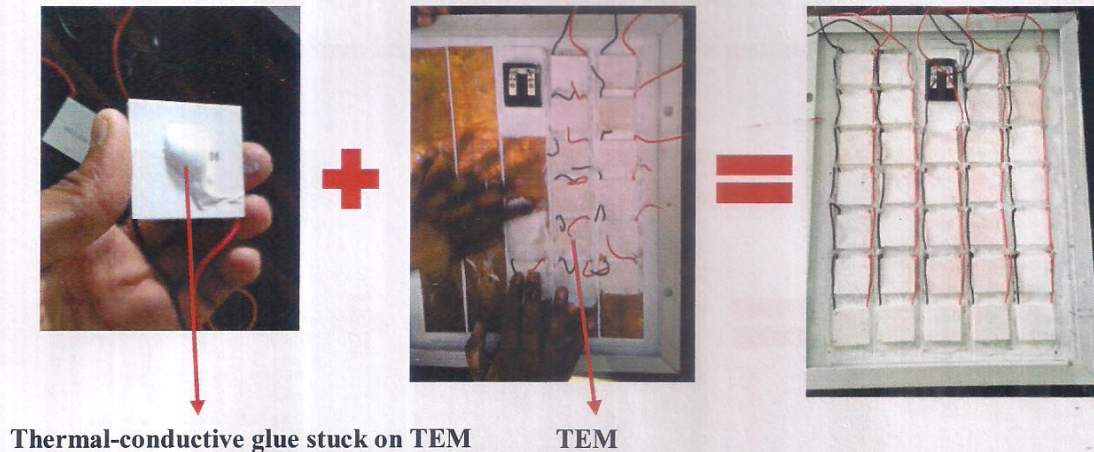
Fig. 3.6 Stepwise attachment of TEM on copper strips attached on PVM

"TEC1-12706" Thermoelectric Module has been used. The dimensions and others parameter of "TEC1-12706" for Bismuth Telluride (Bi_2Te_3) material is given below in Table-3.5.

Parameters	Symbol	Values
Length of module	L_{TE}	40 ± 0.1 mm
Width of module	W_{TE}	40 ± 0.1 mm
Height of module	t_{TE}	3.8 ± 0.1 mm
Area of module	A_{TE}	1600 mm^2
Internal electric resistance	R_{TE}	1.712×10^{-2} Ω (ohm)
Thermal conductance	κ_{TE}	3.564×10^{-2} W/K
Figure of merit	Z	1.6×10^{-3} K^{-1}
Number of TE modules	N_{TE}	33
Number of p-n pair	N	127

Table-3.5 Dimensions and others parameter of "TEC1-12706" for Bismuth Telluride

(iii) In the third step, paraffin wax as a phase-change material (PCM) has been used to fill the gap between TEMs so that no entrapping of air is taking place and also to absorb the heat from these gaps (Fig. 3.7). And finally Al-fins are attached on the TEM with thermal-conductive glue (Fig. 3.9).

n-Heptacosane (C27) Paraffin wax has been poured into gaps beside of TEMs up to the height of TEM (3.8mm height) by melting it. It has a melting point of 59°C, and latent heat 236 kJ/ kg.

Gaps between TEMs   **Melting Paraffin wax**   **Pouring of melting wax in gaps**   **Solidified Paraffin wax**

Fig. 3.7 Stepwise filling of gaps between TEMs by Paraffin wax
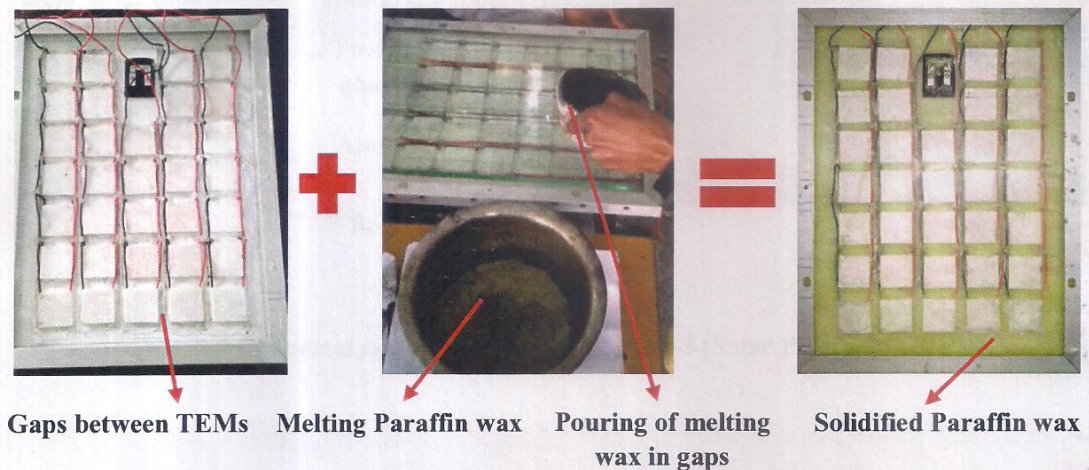
3-D model of Module-3 as shown in fig. 3.8 and Graphical and actual picture of Module-3 (Solar PV-TE Module) as shown below in fig. 3.9 and
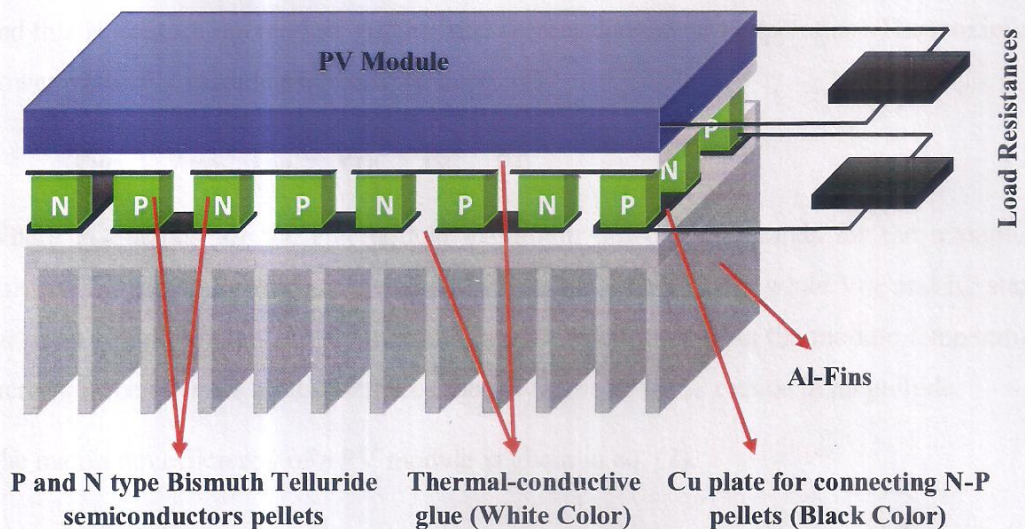

P and N type Bismuth Telluride semiconductors pellets   **Thermal-conductive glue (White Color)**   **Cu plate for connecting N-P pellets (Black Color)**

Fig. 3.8 3-D Model of Module-3 (Solar PV-TE Module)
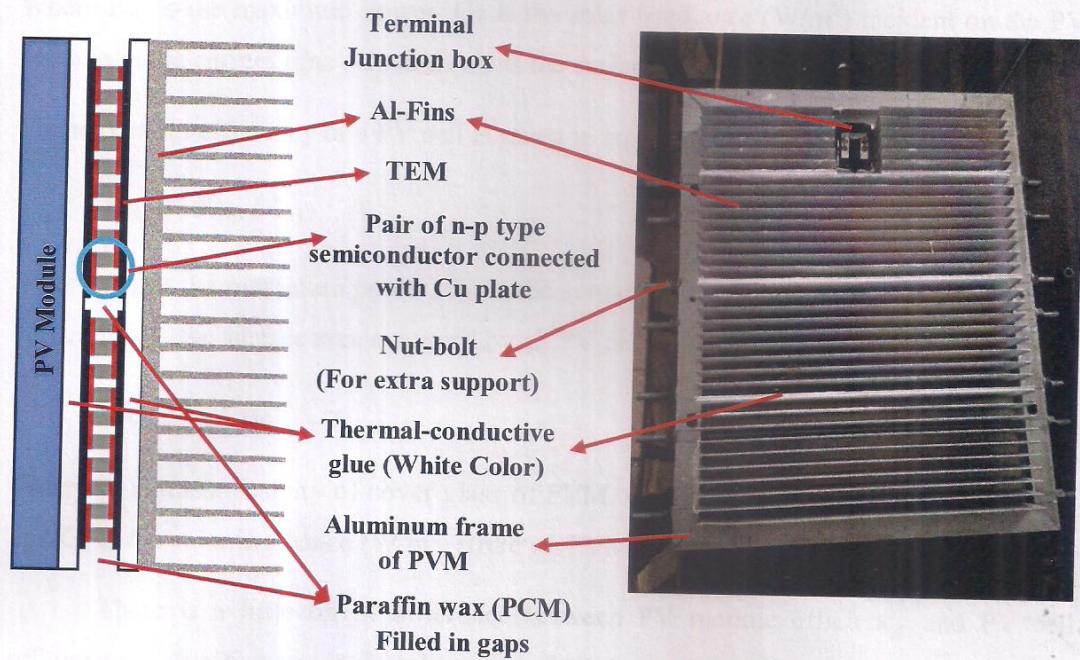
Fig. 3.9 Graphical and Actual picture Module-3 (Solar PV-TE Module)

Labels in the figure:
- Terminal Junction box
- Al-Fins
- TEM
- Pair of n-p type semiconductor connected with Cu plate
- Nut-bolt (For extra support)
- Thermal-conductive glue (White Color)
- Aluminum frame of PVM
- Paraffin wax (PCM) Filled in gaps
- PV Module

3.2 Theory and Analysis:

3.2.1 Electrical Analysis of PV Module:
Power and the efficiency of the PV Module strongly depends on ambient temperature, as well as the temperature of the module and this is because the module voltage and current depend on temperature. The maximum power of the PV module expressed as in eq. (1)

$$P_{mp} = V_{mp} \cdot I_{mp} = V_{OC} \cdot I_{SC} \cdot FF \tag{1}$$

Where P_{mp} stands for the PV module maximum power, V_{mp} stands for the maximum voltage, I_{mp} stands for maximum current, FF stands for fill factor while V_{OC} and I_{SC} stand for open circuit voltage and short circuit current respectively. As the module temperature increases, the I_{SC} rises a little bit while the fill factor and V_{OC} reduce in magnitude.

The maximum efficiency of a PV module is given in eq. (2).

$$\eta_{mp} = P_{mp} / G_T \cdot A_{PV} \tag{2}$$

Where P_{mp} is the maximum power, G_T is the solar irradiance (W/m^2) incident on the PV Module in the current time step and A_{PV} is the surface area of the module in m^2.

The maximum efficiency of a PV cell is given in eq. (3).

$$\eta_{mc} = P_{mp} / G_O \cdot A_c \tag{3}$$

Where P_{mp} is the maximum power, G_O is the actual solar irradiance (W/m^2) strike on PV cell and A_c is the surface area occupied by all PV cells in m^2.

$$G_O = \tau_g \cdot \alpha_c \cdot G_T \tag{4}$$

Where τ_g is transmissivity of cover glass of PVM, α_c is absorptivity of PV cell (Si-cell), and G_T is the solar irradiance (W/m^2) strike on PVM.

There is a little bit of difference between PV module efficiency and PV cell efficiency. Cell efficiency is slightly greater than the module efficiency because the solar radiation strikes on the cell by passing through the cover glass due to this some part of the radiation is reflected by cover glass and PV Si-cell, and another reason is that the surface area of cells is less than the surface area module. In the actual module, efficiency is considered and PVM rated from module efficiency too. In whole experimentation, module efficiency has been calculated but in thermal analysis (will be discussed ahead) cell efficiency is taken for finding the energy input given to TEM.

The temperature effect on a PV module power can be expressed using the equation for PV array power output as in eq. (5)

$$P_{PV} = Y_{PV} \cdot f_{PV} (G_T / G_{T,STC})[1 + \beta(T_c - T_{c,STC})] \tag{5}$$

Where, Y_{PV} ($P_{max,STC}$) is the rated capacity of the PV array, which implies that its output power under standard test conditions (W),

f_{PV} is the PV derating factor (derating factor of 0.9 implies that the test yielded power readings at STC, which are 10% lower than the nameplate rating of the PV manufacturer),

G_T is the solar radiation incident on the PV Module in the current time step (W/m^2),

$G_{T,STC}$ is the incident radiation at Standard Test Conditions (1000 W/m^2),

β is the temperature coefficient of power (-0.43 %/°C for polycrystalline Si-cell)

T_c is the PV cell temperature in the current time step (°C)

$T_{c,STC}$ is the PV cell temperature under standard test conditions (25°C)

48

The temperature effect on a PV module efficiency expressed as in eq. (6)

$$\eta_{PV} = \eta_{PV,STC} [1 + \beta(T_c - T_{c,STC})] = P_{PV} / (G_T \cdot f_{PV} \cdot A_{PV}) \qquad (6)$$

Where $\eta_{PV,STC}$ is the PV module's efficiency under standard test condition (%).

$$\eta_{PV,STC} = Y_{PV} / (G_{T,STC} \cdot A_{PV}) \qquad (7)$$

Similarly, the efficiency of the PV cell can also be written by replacing the G_T and A_{PV} with G_O and with A_c.

3.2.2 Electrical Analysis of TE Module:

Power and the efficiency of the TE Module depends on the temperature of hot and cold side of TE module, and this is because the module voltage and current depend on temperature. The maximum power of the TE module expressed as in eq. (8)

$$P_{TE} = V_{TE} \cdot I_{TE} \qquad (8)$$

Where P_{TE} stands for the TE module maximum power, V_{TE} stands for the maximum voltage, and I_{TE} stands for maximum current.

The maximum efficiency of a TE module is given in eq. (9).

$$\eta_{TE} = P_{TE} / Q_{H,TE} \qquad (9)$$

Where P_{TE} is the maximum power, $Q_{H,TE}$ is the heat input to the TEM or heat supplied to hot side of TEM.

The temperature effect on a TE module power can be expressed as in eq. (10)

$$P_{TE} = Q_{H,TE} \cdot \eta_{car} [(M - 1) / (M + (T_{C,TE} / T_{H,TE})] \qquad (10)$$

$$M = \sqrt{(1 + ZT_m)}, \quad T_m = 0.5(T_{H,TE} + T_{C,TE}), \quad \eta_{car} = (T_{H,TE} - T_{C,TE}) / T_{H,TE}$$

Where Z is the figure of merit (K^{-1}),

$T_{H,TE}$ and $T_{C,TE}$ are the hot and cold side temperatures of TE module respectively (K),

T_m is the average temperature (K), η_{car} is the Carnot efficiency.

The power of TEM can also be written as in eq. (11)

$$P_{TE} = Q_{H,TE} - Q_{C,TE} = N \cdot N_{TE} \cdot (I_{TE})^2 \cdot R_L \tag{11}$$

Where $Q_{H,TE}$ is the heat input to the TEM or heat supplied to hot side of TEM, $Q_{C,TE}$ is the heat rejected to the ambient from the cold side of TEM, N is the total no. of n-p pair in one TEM, N_{TE} is the no. of TEM, I_{TE} stands for maximum current, and R_L is the load resistance.

$Q_{H,TE}$ and $Q_{C,TE}$ can be calculate using eq. (12) and (13).

$$Q_{H,TE} = N \cdot N_{TE}[S_{TE} \cdot I_{TE} \cdot T_{H,TE} - 0.5 \cdot (I_{TE})^2 \cdot R_{TE} + \kappa_{TE}(T_{H,TE} - T_{C,TE})] \tag{12}$$

Only a small part of waste heat ($Q_{H,TE}$) can be converted to power by TEM and the rest part, $Q_{C,TE}$, flows through the back side to the ambient and can be expressed as follows

$$Q_{H,TE} = N \cdot N_{TE} [S_{TE} \cdot I_{TE} \cdot T_{H,TE} + 0.5 \cdot (I_{TE})^2 \cdot R_{TE} + \kappa_{TE}(T_{H,TE} - T_{C,TE})] \tag{13}$$

Where N is the total no. of n-p pair in one TEM, N_{TE} total no. of TEM, I_{TE} stands for maximum current, and R_{TE} is internal electric resistance of p-n pair, κ_{TE} is thermal conductance (W/K)

Besides of this $Q_{H,TE}$ can be calculate by doing thermal analysis of PV module (will be discussed ahead) and $Q_{H,TE}$ has been calculated from thermal analysis in whole experimentation.

3.2.3 Thermal Analysis of PV Module: To calculate Heat input to TEM i.e., $Q_{H,TE}$, thermal analysis of PV Module has been done.

When the solar radiation incident on the PVM, some part is reflected and absorbed by the cover glass and 90% part of solar radiation is incident on the PV cell. Out of this 90% radiation, 85% part is absorbed by the PV cell which is actual energy input to PVM and it is given below in eq. (14).

$$E_{in} = \tau_g \cdot \alpha_c \cdot G_T \cdot A_{PV} \tag{14}$$

Where τ_g is the transmissivity of cover glass represents (0.90), α_c is the absorptivity of PV cell (0.85), G_T is the solar irradiance (W/m^2) incident on the PV Module in the current time step and A_{PV} is the surface area of the module in m^2.

It is assumed that convective and radiative heat is lost from the top surface of PVM to the ambient. Besides this convection also take place from the bottom of Tedlar and

contributed to heat input of TEM. Here only heat lost from the top surface is calculated as given below in eq. (15) and eq. (16).

$$Q_{conv} = h_c \cdot A_c \cdot (T_c - T_a) \tag{15}$$

$$Q_{rad} = \varepsilon_c \cdot \sigma \cdot A_c \cdot (T_c^4 - T_{sky}^4) \tag{16}$$

Where T_a represents the ambient temperature,

σ is the Stefan–Boltzmann constant and is equal to 5.67×10^{-8} (W/m^2 K^4),

ε_c is the emissivity (0.88 for Si-cell) of PV cell, A_c is the total surface area of cells,

T_{sky} is the effective temperature of the sky and it is calculated by considering the sky as a black body is given by $\quad T_{sky} = 0.0552 \times T_a^{1.5}$

h_c is the average heat transfer coefficient between PV cell and the ambient and it is given by the expression $\quad h_c = 2.8 + 3 \cdot u_w$, Where u_w (m/s) represents the speed of wind.

Now applying energy balance to find out the heat input for TEM.

$$E_{in} = P_{mp} + Q_{conv} + Q_{rad} + Q_{ted} \tag{17}$$

Where P_{mp} is the maximum power of PV module, Q_{ted} is the energy transfer to tedlar and one part of this is used as input ($Q_{H,TE}$) of TEMs as in eq. (18) and remaining part is absorbed (Q_{wax}) by paraffin wax (PCM).

$$Q_{ted} = Q_{H.TE} + Q_{wax} \quad \gg \quad Q_{H.TE} = Q_{ted} (N_{TE} \cdot A_{TE} / A_{PV}) \tag{18}$$

Where N_{TE} total no. of TEM, A_{TE} surface area of TEMs, and A_{PV} surface area of PVM.

On substituting the values of E_{in}, P_{mp}, Q_{conv}, Q_{rad} from equations (1), (14), (15), and (16) in the above eq. (17) Q_{ted} can be calculated and further from eq. (18) the heat input for TEM ($Q_{H,TE}$) can also be calculated.

$Q_{H,TE}$ can also be calculated by considering the thermal conductive resistance in the PV module and the Tedlar, then $Q_{H,TE}$ is expressed as in eq. (19)

$$Q_{H,TE} = (T_c - T_{H,TE}) \left[t_c / (k_c \cdot A_c) + t_{ted} / (k_{ted} \cdot A_{PV}) \right]^{-1} \tag{19}$$

Where T_c is the cell temperature, $T_{H,TE}$ is the hot side temperature of TEM, k_c and k_{ted} are the thermal conductivity of the PV cell and the Tedlar respectively, t_c and t_{ted} are their corresponding thicknesses. A_c and A_{PV} are the surface area of PV cells and module respectively.

Thermal analysis of PVM is represented in the form of energy distribution in PVM in fig. 3.10
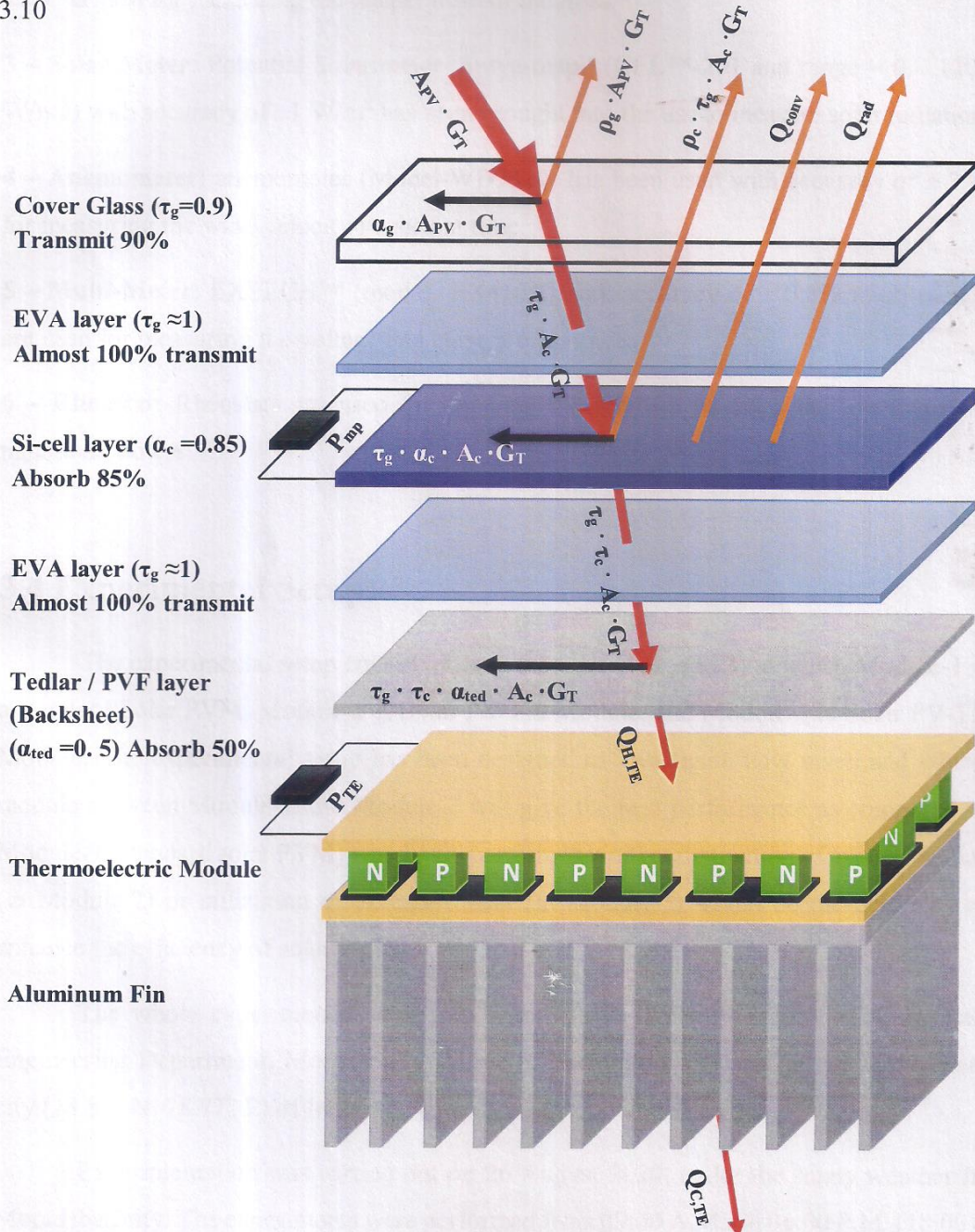

Fig. 3.10 Thermal Analysis of the PVM in the form Energy Distribution in PVM

Dr. Munish Chhabra
Professor & Head
Deptt. of Mechanical Engg.
Moradabad Institute of Technology
Moradabad - 244001

3.3 Apparatus used in Experiment:

1 - Thermal Imaging Camera: "testo 865" thermal imaging camera with accuracy of ±2°C is used for taking thermal pictures and measuring the temperature of modules.

2 – Infrared Thermometer: "EXTECH 42545" infrared thermometer with accuracy of ±2°C is used for measuring the temperature of modules.

3 – Solar Meter: Potential Solarimeter 'Surya-mapi' (CEL™-201 and range = 0 – 1200 W/m2) with accuracy of ±1 W/m^2 has been brought into the use to measure solar radiation.

4 – Anemometer: anemometer (Model-WD9819) has been used with accuracy of ± 3%. for measuring the wind velocity in current time.

5 – Multi-Meter: EXTECH™ (model- EX410A) with accuracy of ± 0.5% multi-meters are used for measuring the voltage and current of modules.

6 – Rheostat: Rheostats are used for applying the load on modules and set them for maximum power.

3.4 Experimental Setup:

The experimental setup consist of three modules (1, 2, and 3) in which Module-1 is a standard Solar PVM, Module-2 is Solar PV-Fin Module, and Module-3 is Solar PV-TE Module. The experimental setup has been designed to investigate how much and which module between Module-2 and Module-3 will give the best performance as compared to Module-1 (standard solar PVM) which will confirm that either dissipation of excessive heat (in Module-2) or utilization of excessive heat (in Module-3) would be the best way to enhance the efficiency of solar PVM.

The whole experimental setup was installed on the rooftop of the Mechanical Engineering Department, Moradabad Institute of Technology, located in the Moradabad city (28.83° N, 78.77° E) of India.

Experimentation was carried out on 26 August 2020, under the sunny weather in Moradabad city. The experiments were performed from 09:00 A.M. till 06:00 P.M. (18:00), and all the three modules (Module-1, Module-2, and Module-3) were placed in parallel to each other facing south at angle 28.83°, as shown in fig. 3.11 and fig. 3.12. Furthermore,

two multi-meters with one rheostat are connected with each module, in such a way that the first multi-meter represents a voltage and connected in parallel, and the second multi-meter represents a current and connected in series. Accordingly, the time was adjusted, and every 30 minutes the temperatures were recorded for all the modules by using the infrared thermometer, and pictures were captured by thermal imaging camera. Meanwhile, the rheostat was adjusted to obtain maximum voltage and maximum current to optimize the obtained power. In every 30 minutes time interval, the irradiation and wind speed was also measured by using solar meter and anemometer respectively.
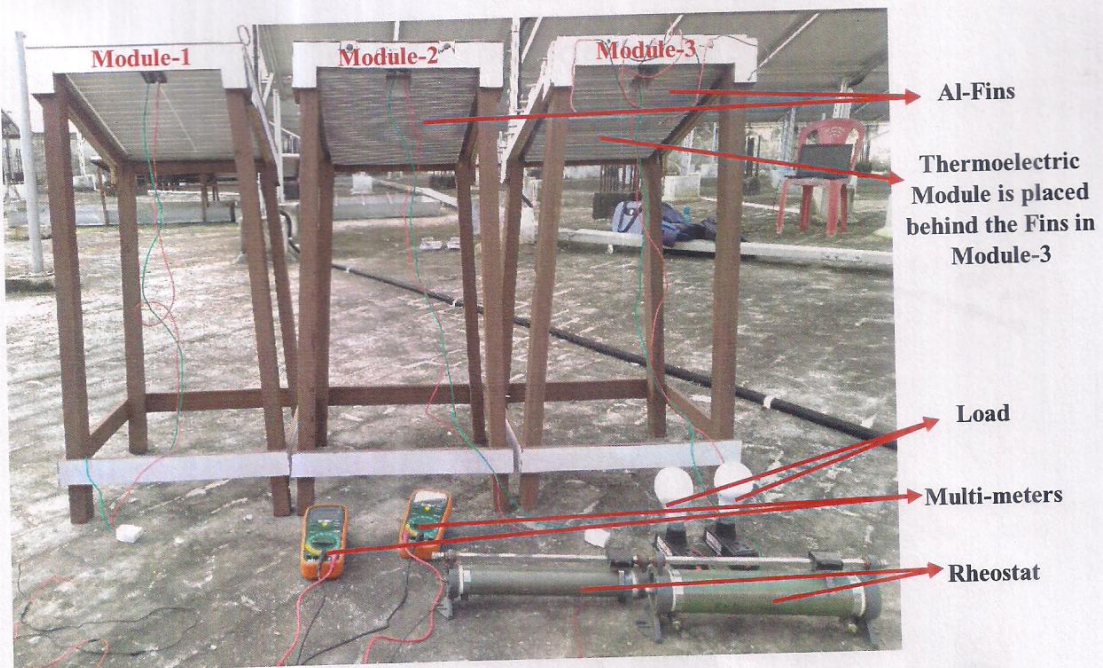

Fig. 3.11 Experimental setup Front view

Fig. 3.12 Experimental setup Rear view

Chapter-4
Results and Discussion

■■■■■■■

This experimental work was conducted to analyze the effect on the performance of the PVM with the dissipation of heat in Module-2 and the utilization of heat in Module-3, and they were compared with standard PVM. Results were recorded from all modules simultaneously and the following relation among different parameters was found that affect the performance of PVM.

4.1 Solar Radiation variation with Time :

Solar Radiation intensity has been recorded between time interval 09:00 A.M. to 06:00 P.M. (18:00) with the help of Solar-meter and the variation of solar radiation intensity with time shown in the graph (Fig. 4.1)
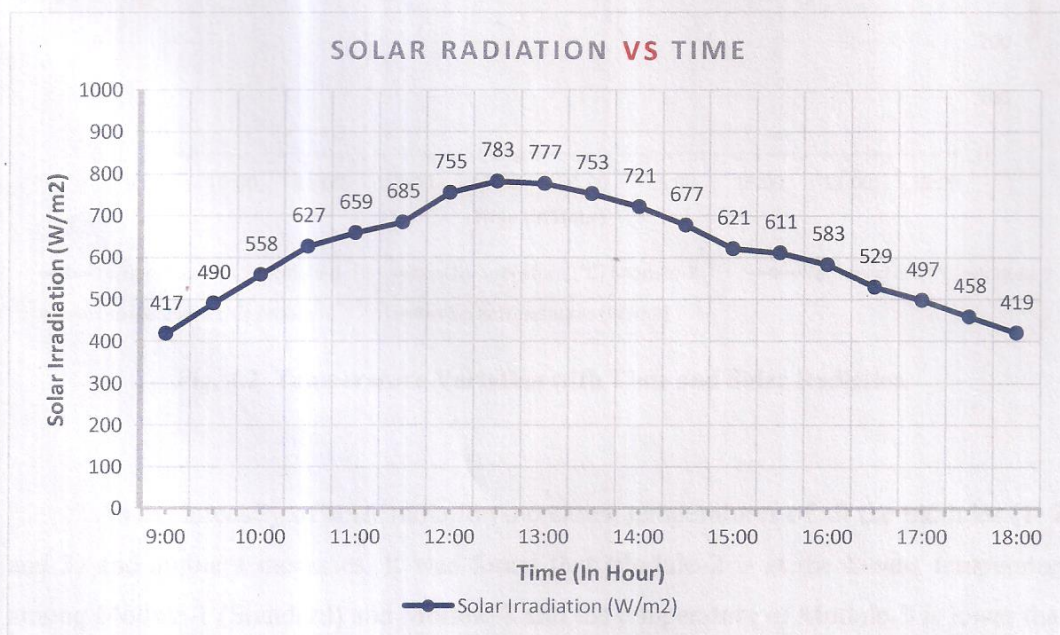

SOLAR RADIATION VS TIME

Fig. 4.1 Solar Radiation Variation with Time

During the rising of the sun the intensity of solar radiation increases at a high rate till 11:30 A.M. and at a low rate till 12:30 P.M with a maximum of 783 W/m². After that, it decreases slowly till 2:30 P.M. and then decreases at high rate. Sun reaches to its peak in between 12:00 P.M to 1:30 P.M.

4.2 Temperature variation with Time and Solar Radiation :

Temperatures of all the three modules (1, 2, and 3) and ambient were recorded over the time interval 09:00 A.M. to 06:00 P.M. (18:00) and solar radiation with the help of Infrared thermometer shown in graph (Fig. 4.2) and thermal picture also taken by the Thermal imaging camera shown in figure (Fig. 4.3).
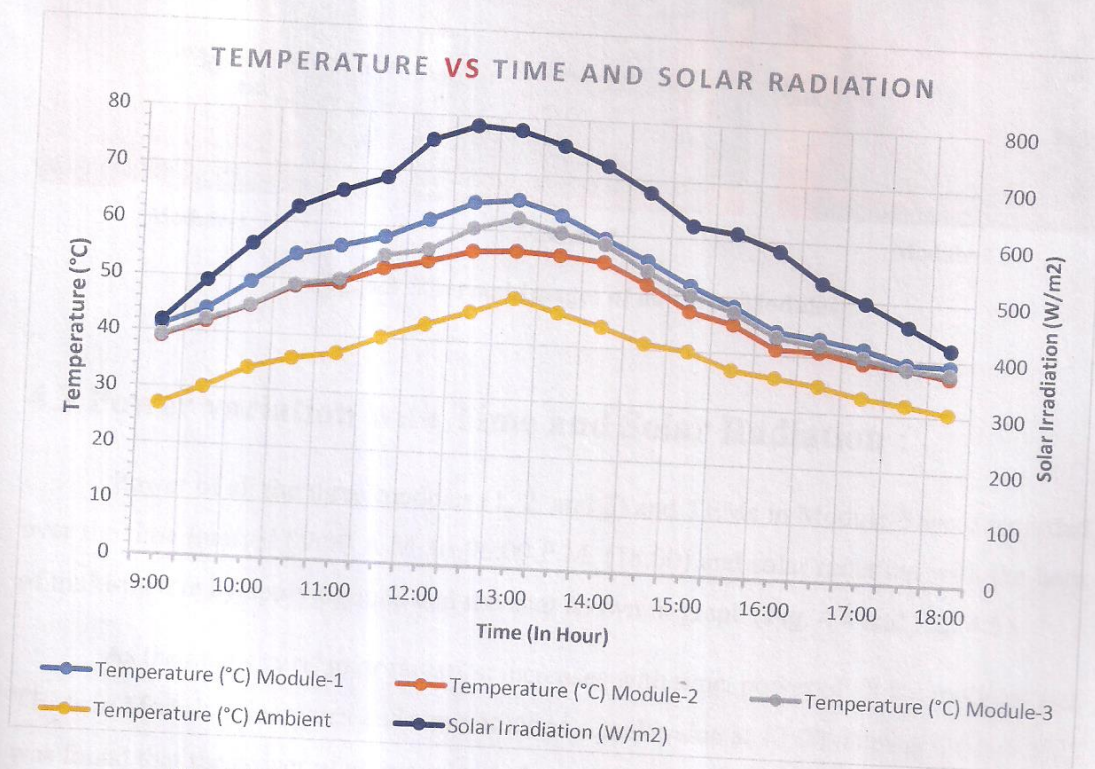

Fig. 4.2 Temperature Variation with Time and Solar Radiation

As the intensity of solar radiation increases, temperatures of all the modules (1, 2, and 3) and ambient increases. It was found that Module-2 is at the lowest temperature among Module-1 (Standard) and Module-3 and the temperature of Module-3 is lower than Module-1. The graph shows that the maximum temperatures of Module-1, 2, and 3 were

found at 65.4 °C, 56.4 °C, and 62.3 °C respectively at 13:00. Due to the attachment of Al-fin on Module-2 and Module-3, a significant increase in the heat transfer rate was found that result in a reduction in the temperature in comparison to Module-1 (Standard). And the PCM in Module-3 stored the thermal energy in the form of latent heat of vaporization that results in a slight increase in the temperature than Module-2 and reduces in comparison of Module-1.

The average percentage reduction in the temperature of Module-2 and Module-3 was found 8.7% and 4.97% respectively with Module-1 (Standard) and percentage reduction in the temperature of Module-2 was found 3.92% as compared to Module-3, i.e., Module-2 was found to be more effective among Module-1 and Module-3.
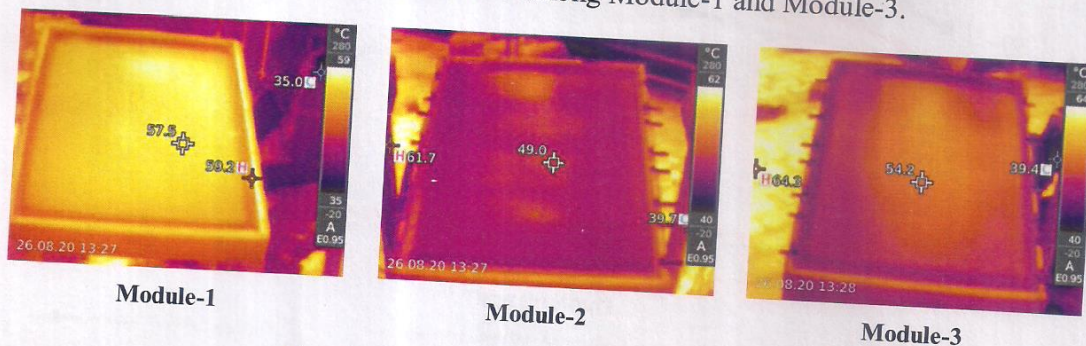

Fig. 4.3 Thermal Images of all three Modules

4.3 Power variation with Time and Solar Radiation :

Power of all the three modules (1, 2, and 3) and TEMs in Module-3 were recorded over the time interval 09:00 A.M. to 06:00 P.M. (18:00) and solar radiation with the help of multi-meters by applying load and rheostat shown in graph (Fig. 4.4 and Fig. 4.5).

As the intensity of solar radiation increases with time, power of all the modules and TEMs in Module-3 increases and were attained a peak value at 13:00. During the testing it was found that the power of all modules 1, 2, and 3 attains a maximum value of 13.932 W, 16.102 W, and 15.675W respectively, and the power of TEMs was found 0.838 W that is very small because of the low performance and unfavorable condition of thermoelectric modules. During the testing, a significant increase in power of Module-2 was found among Module-1 and Module-3 i.e., Module-2 is more effective than Module-1 and Module-3.

The average percentage increment in the power of Module-2 and Module-3 was found 14.42% and 8.72% respectively with Module-1 (Standard) and percentage increment

in the power of Module-2 was found 5.24% as compared to Module-3, i.e., Module-2 was found to be more effective in power output among Module-1 and Module-3 (Fig. 4.4).

Overall maximum power of Module-3 (incuding TEMs) was found 16.513W and average power is approximately same as (Slightly less) Module-2 (Fig. 4.5).
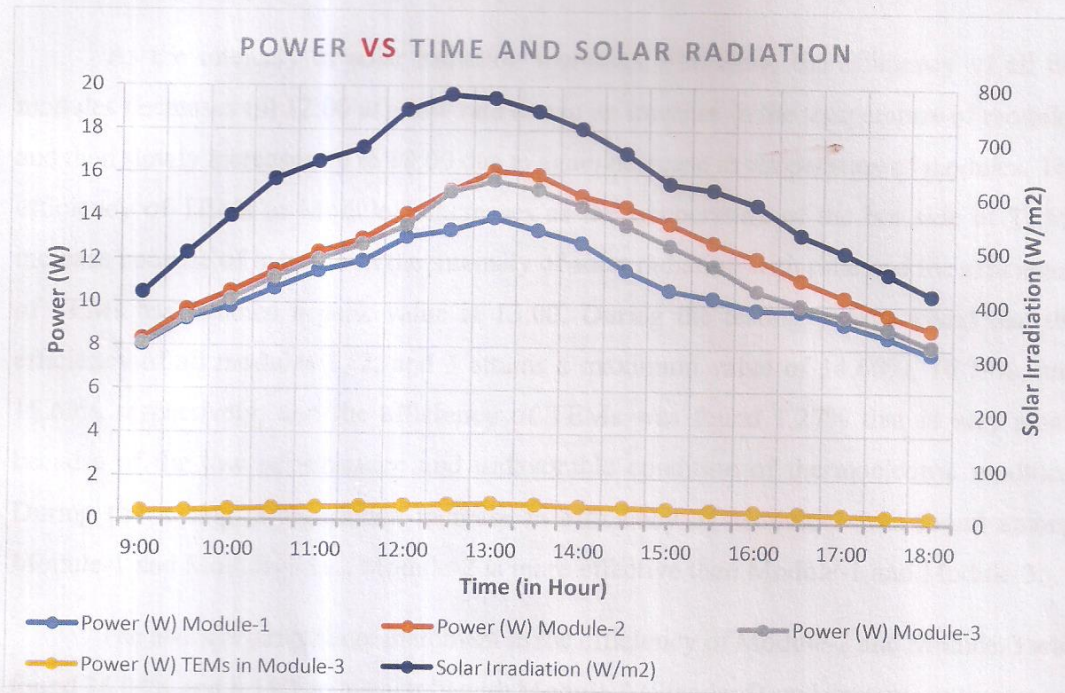

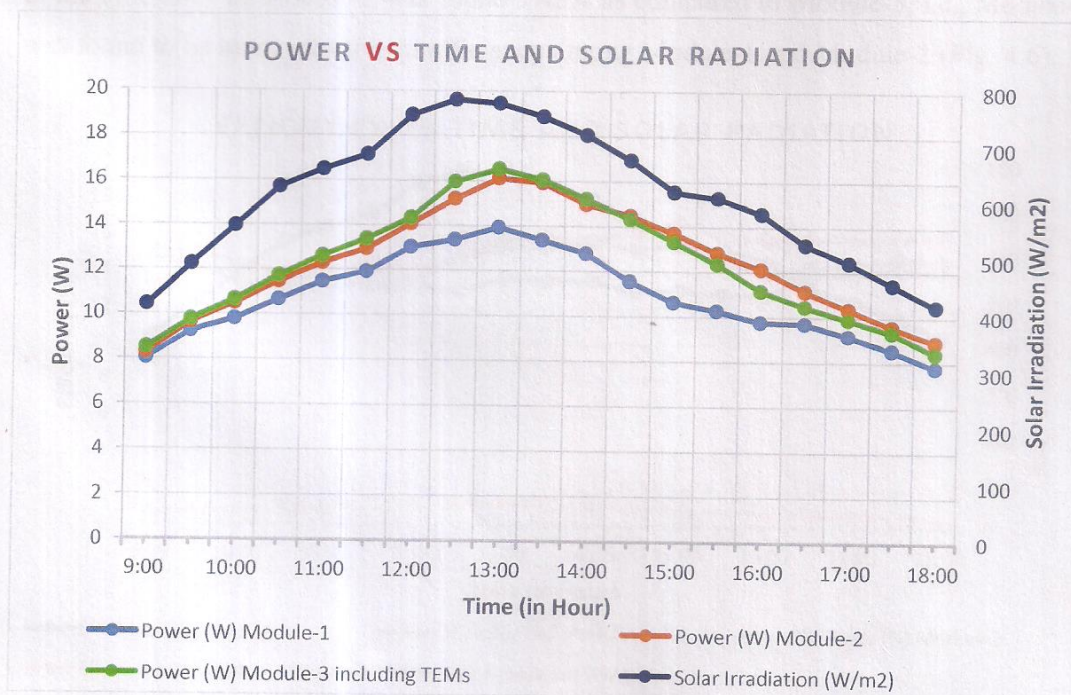**Fig. 4.4 Power Variation with Time and Solar Radiation**

Fig. 4.5 Power Variation with Time and Solar Radiation

4.4 Efficiency variation with Time and Solar Radiation :

The efficiency of all three modules (1, 2, and 3) and TEM in Module-3 were recorded over the time interval from 09:00 A.M. to 06:00 P.M. (18:00) and solar radiation shown in graph (Fig. 4.6 and Fig. 4.7).

As the intensity of solar radiation increases with time, the efficiency of all the modules decreases till 12:00 at a low rate due to an increase in the temperature of modules and then slowly increases up to 18:00 due to again decrease in temperature of modules. The efficiency of TEMs in Module-3 increases as the temperature of the hot side of TEMs increase because of increase in the intensity of solar radiation with time and the efficiency of TEMs has attained a peak value at 13:00. During the testing, it was found that the efficiency of all modules 1, 2, and 3 attains a maximum value of 14.66%, 16.79%, and 15.63% respectively, and the efficiency of TEMs was found 1.27% that is very small because of the low performance and unfavorable condition of thermoelectric modules. During the testing, a significant increase in efficiency of Module-2 was found among Module-1 and Module-3 i.e., Module-2 is more effective than Module-1 and Module-3.

The average percentage increment in the efficiency of Module-2 and Module-3 was found 14.04% and 8.18% respectively with Module-1 (Standard) and percentage increment in the efficiency of Module-2 was found 5.42% as compared to Module-3, i.e., Module-2 was found to be more effective in efficiency among Module-1 and Module-3 (Fig. 4.6).
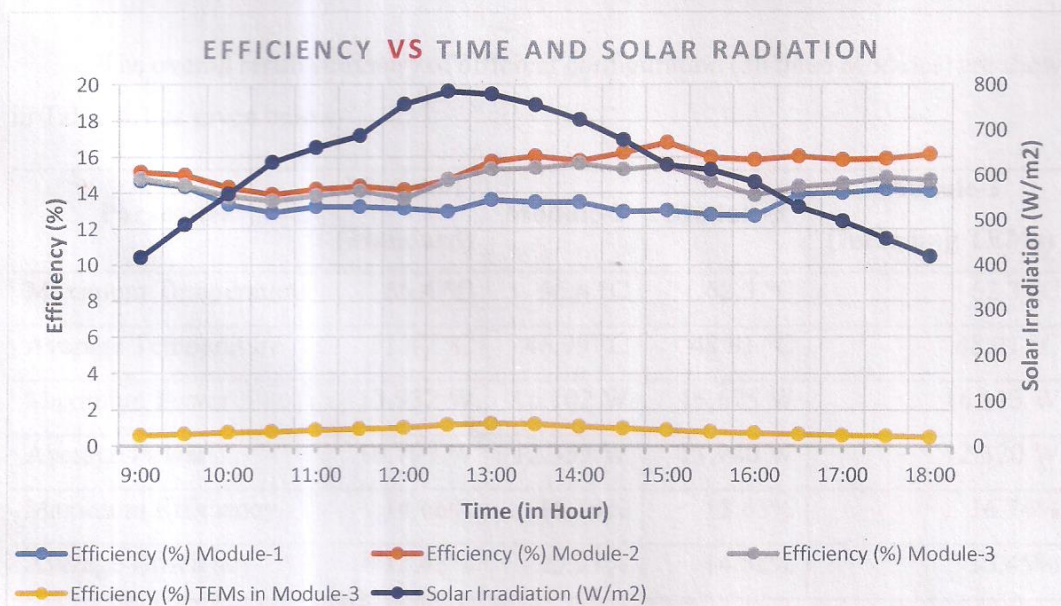

Fig. 4.6 Efficiency Variation with Time and Solar Radiation

Overall maximum efficiency of Module-3 (Including TEMs) has been found 16.74% and an increment in the average efficiency of Module-3 (including TEMs) was found 14.62% and 0.503% (Approx. 0%) as compared to Module-1 and Module-2 respectively (Fig. 4.7) i.e., there is no significant difference in the efficiency of Module-2 and Module-3 (including TEMs).
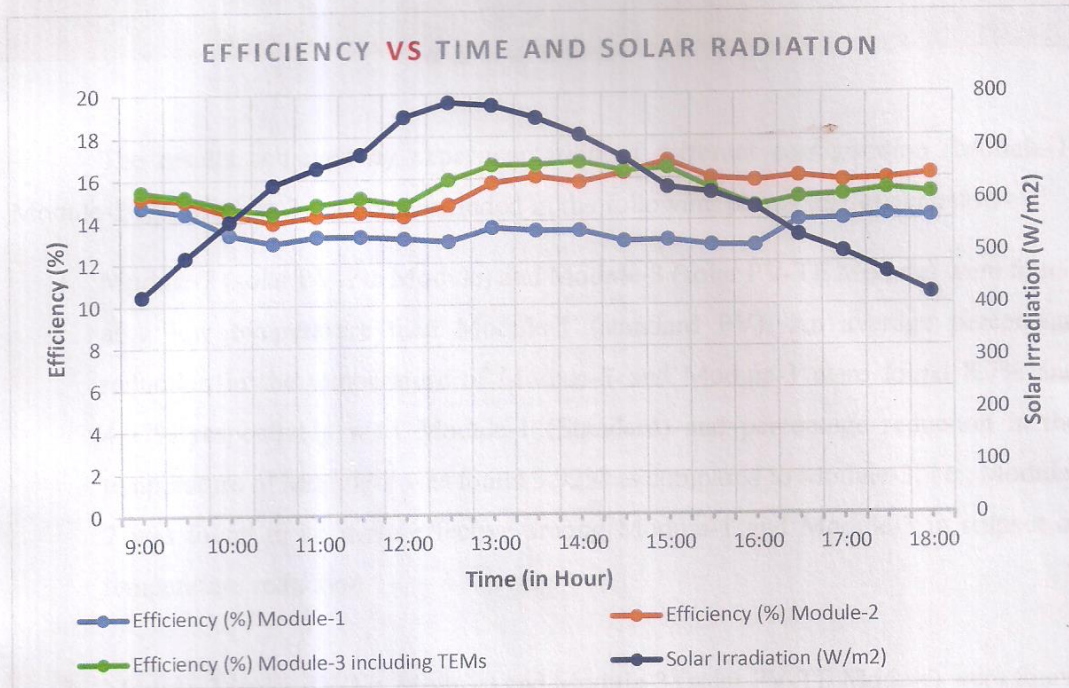
Fig. 4.6 Efficiency Variation with Time and Solar Radiation

The overall result summary of different configuration (all three Modules) are shown in Table 4.1 as given below-

Parameter	Module-1 (Standard)	Module-2	Module-3	Module-3 (Including TEMs)
Maximum Temperature	65.4 °C	56.4 °C	62.3 °C	62.3 °C
Average Temperature	51.47 °C	46.99 °C	48.91 °C	48.91 °C
Maximum Power	13.932 W	16.102 W	15.675 W	16.513 W
Average Power	10.797 W	12.353 W	11.740 W	12.320 W
Maximum Efficiency	14.66%	16.79%	15.63%	16.74%
Average Efficiency	13.48%	15.37%	14.58%	15.45%

Table 4.1 Overall result summary of all three modules

Chapter-5
Conclusions

The results achieved by experimentation of different configuration (Module-1, Module-2 and Module-3) can be concluded in the following points that given below-

1. Module-2 (solar PV-Fin Module) and Module-3 (solar PV-TE Module) were found at a low temperature than Module-1 (standard PV). An average percentage reduction in the temperature of Module-2 and Module-3 were found 8.7% and 4.97% respectively w.r.t Module-1 (Standard) and percentage reduction in the temperature of Module-2 was found 3.92% as compared to Module-3, i.e., Module-2 was found to be more effective among Module-1 and Module-3 in respect of temperature reduction.

2. Module-2 (solar PV-Fin Module) and Module-3 (solar PV-TE Module) were found in the significant-high power output than Module-1 (standard PV). An average percentage increment in the power of Module-2 and Module-3 were found 14.42% and 8.72% respectively with Module-1 (Standard). TEMs in Module-3 showed maximum power of 0.838 W that is very small because of the low performance and unfavorable condition of thermoelectric modules. So overall maximum power of Module-3 (including TEMs) was found 16.513W and the average power was approximately the same as (Slightly less) Module-2. The average percentage increment in the power of Module-2 was found 5.24% w.r.t. Module-3 (excluding TEMs) and 0.267% (Approx. 0%) w.r.t. Module-3 (including TEMs), i.e., again Module-2 is best among Module-1 and Module-3 in respect of power.

3. Module-2 (solar PV-Fin Module) and Module-3 (solar PV-TE Module) have been found at high efficiency than Module-1 (standard PV). An average percentage increment in the efficiency of Module-2 and Module-3 were found 14.04% and

8.18% respectively w.r.t Module-1 (Standard). TEMs in Module-3 showed maximum efficiency of 1.27% that is very small because of the low performance and unfavorable condition of thermoelectric modules. Overall maximum efficiency of Module-3 (including TEMs) was found 16.74% and average efficiency was approximately the same as (Slightly less) Module-2. The average percentage increment in the efficiency of Module-2 was found 5.42% as compared to Module-3 (excluding TEMs) and Approx. 0% as compared to Module-3 (including TEMs), i.e., again Module-2 is best among Module-1 and Module-3 in respect of efficiency.

The overall conclusion of all the above three-point is that Module-2 is the best module over Module-1 and Module-3 in respect of temperature, power and efficiency.

Module-3 (including TEMs) gives the same performance as Module-2, i.e., dissipation and utilization of heat in Module-2 (solar PV-Fin Module) and Module-3 (solar PV-TE Module) enhance the performance of PVM by the same amount, therefore final conclusion arises that dissipation heat in Module-2 with the help of Al-fins is the best way to enhance the performance of PVM rather than the utilization of heat by TEMs in Module-3. In short, Module-2 (Solar PV-Fin Module) gives a better performance compared to Module-3 (Solar PV-TE Module) because of the low efficiency of TEMs (approx. 5-6%) and lack of favorable condition for TEMs in Module-3, that is why Module-3 lagging with Module-2 to enhance the performance of PVM.

Future Scope

■■■■■■■

As has been found in the conclusions that dissipation and utilization of heat in Module-2 and Module-3 enhances the performance of PVM but at the same time it was found that the dissipation of heat is the best way to enhance the performance of PVM rather than the utilization of heat. In short, Module-2 (Solar PV-Fin Module) gives a better performance compared to Module-3 (Solar PV-TE Module) because of the use of TEM in Module-3. In Solar PV-TE Hybrid System (Module-3), TEM was used to utilize the waste heat of PVM, and from the literature review, the efficiency of TEM is about 5-6% that means only 5-6% part of waste heat would be converted into electricity, that is why Module-3 lagging with Module-2 to enhance the performance of PVM.

To ensure the efficient working of the "Solar PV-TE Hybrid System" the efficiency of the thermoelectric module plays a crucial role. Therefore, the scope of the future is to ensure the efficient working of the Solar PV-TE Hybrid System by working on the material of the thermoelectric module so that it leads the Module-2. Currently, Bismuth Telluride (Bi_2Te_3) and Lead Telluride (PbTe) semiconductor materials are being used in the fabrication of a thermoelectric module. Continual researches are going on to develop such type of material which is highly thermoelectric, so it has been found that it has the potential of acquiring an efficiency of 15%, which has demonstrated by the development of new thermoelectric material made-up of Cobalt-Antimony. In this series, it is observed by the experimental study that Nanotechnology can become the best option to use as a thermoelectric material instead of a semiconductor.

Dr. Munish Chhabra
Professor & Head
Deptt. of Mechanical Engg.
Moradabad Institute of Technology
Moradabad - 244001

References

[1] **Book -** *Heat and Mass Transfer: Fundamentals and Applications:* By Y. A. Çengel and A. J. Ghajar. 4th edition: McGraw-Hill, New York 2011.

[2] **Book -** *Thermodynamics: An Engineering Approach:* By Yunus A. Çengel, Michael A. Boles. 8th edition: McGraw-Hill, New York 2015

[3] **Book -** *Alternative Energy Sources :* By Efstathios E. (Stathis) Michaelides.: Springer-Verlag Berlin Heidelberg 2012

[4] **Book -** *Solar PV and Wind Energy Conversion Systems: An Introduction to Theory, Modeling with MATLAB/SIMULINK, and the Role of Soft Computing Techniques:* By S. Sumathi • L. Ashok Kumar • P. Surekha. : Springer International Publishing Switzerland 2015

[5] Solar Panel and Solar cell efficiency – Wikipedia

[6] Thermoelectric effect, Thermoelectric generator, and Thermoelectric materials - Wikipedia

[7] Heat sink and Fin (Extended Surface) – Wikipedia

[8] Aluminum Heat sink - Radian Thermal Products, Inc.

[9] Thermally Conductive Adhesives – Permabond Engineering Adhesives Ltd.

[10] Thermally Conductive Adhesives – Panacol Adhesives Ltd.

[11] Phase-change material and Paraffin wax – Wikipedia

[12] Amir Reza Vakhshouri, 2019 "Paraffin as Phase Change Material"

[13] Manish K. Rathod, 2018 "Phase Change Materials and Their Applications"

[14] E.Radziemska / Renewable Energy 28 (2003) 1-12, "The effect of temperature on the power drop in crystalline silicon solar cells"

[15] Swapnil Dubey et al. / Energy Procedia 33 (2013) 311 – 321, "Temperature Dependent Photovoltaic (PV) Efficiency and Its Effect on PV Production in the World A Review"

[16] Hongbing Chen et al. / Int. J. of Smart Grid and Clean Energy 3, 4, 2014, 374-379, "Comparative study on the performance improvement of photovoltaic panel with passive cooling under natural ventilation"

[17] E.Skoplaki, J.A.Palyvos / Solar Energy 83 (2009) 614-624, "On the temperature dependence of photovoltaic module electrical performance: A review of efficiency/power correlations"

[18] Erdem Cuce et al. / Int. J. of Low-Carbon Technologies 2011, 6, 299–308, "Effects of passive cooling on performance of silicon photovoltaic cells"

[19] Dengfeng Du / Solar Energy 97 (2013) 238-254, "Thermal management systems for Photovoltaics (PV) installations: A critical review"

[20] Adham Makki et al. / Renewable and Sustainable Energy Reviews 41 (2015) 658-684, "Advancements in hybrid photovoltaic systems for enhanced solar cells performance"

[21] Peter Atkin, Mohammed M.Farid / Solar Energy 114 (2015) 217-228, "Improving the efficiency of photovoltaic cells using PCM infused graphite and aluminium fins"

[22] Leonardo Michelia et al. / Energy Procedia 82 (2015) 301 – 308, "Plate micro-fins in natural convection: an opportunity for passive concentrating photovoltaic cooling"

[23] Cătălin George Popovici et al. / Energy Procedia 85 (2016) 425 – 432, "Efficiency improvement of photovoltaic panels by using air cooled heat sinks"

[24] S. Nižetić et al. / Energy 111 (2016) 211-225, "Experimental and numerical investigation of a backside convective cooling mechanism on photovoltaic panels"

[25] Ahmad El Mays et al. / Energy Procedia 119 (2017) 812–817, "Improving Photovoltaic Panel Using Finned Plate of Aluminum"

[26] S. Nižetić et al. / Energy Conversion and Management 149 (2017) 334–354, "Comprehensive analysis and general economic-environmental evaluation of cooling techniques for photovoltaic panels, Part I: Passive cooling techniques"

[27] Linus Idoko et al. / Energy Reports 4 (2018) 357–369, "Enhancing PV modules efficiency and power output using multi-concept cooling technique"

[28] Qi Luo, Penghui Li et al. / Applied Thermal Engineering 157 (2019) 113666, "Experimental investigation on the heat dissipation performance of flared-fin heat sinks for concentration photovoltaic modules"

[29] U. Sajjad, et al. / Case Studies in Th. Engineering 14 (2019) 100420, "Cost effective cooling of photovoltaic modules to improve Efficiency"

[30] K. P. Amber et al. / J. of Th. Analysis and Calorimetry 2020, "Experimental performance analysis of two different passive cooling techniques for solar photovoltaic installations"

[31] Karim Egab et al. / 2020 IOP Conf. Ser.: Mater. Sci. Eng. 671 012133, "Enhancing a solar panel cooling system using an air heat sink with different fin configurations"

[32] Sandro Nižetić et al. / J. of Th. Analysis and Calorimetry 141 (2020) 163–175, "Analysis of novel passive cooling strategies for free-standing silicon photovoltaic panels"

[33] Parkunam N et al. / Energ Source A. 2020, 42(6), 653–63, "Experimental analysis on passive cooling of flat photovoltaic panel with heat sink and wick structure"

[34] Jaemin Kim et al. / Energies 2020, 13, 85, "Experimental and Numerical Study on the Cooling Performance of Fins and Metal Mesh Attached on a Photovoltaic Module"

[35] Zainal Arifin et al. / Int. J. of Photoenergy 2020, 1574274, 9, "Numerical and Experimental Investigation of Air Cooling for Photovoltaic Panels Using Aluminum Heat Sinks"

Dr. Munish Chhabra
Professor & Head
Deptt. of Mechanical Engg.
Moradabad Institute of Technology
Moradabad - 244001

[36] A.M. Elbreki et al. / Case Studies in Th. Engineering 19 (2020) 100607, "An innovative technique of passive cooling PV module using lapping fins and planner reflector"

[37] Y. Tripanagnostopoulos et al. / Solar Energy 72 (2002) 217-234, "Hybrid photovoltaic/thermal solar systems"

[38] J. K. Tonui, Y. Tripanagnostopoulos / Solar Energy 81 (2007) 498-511, "Air-cooled PV/T solar collectors with low cost performance improvements"

[39] A. S. Joshi et al. / Int. J. of Th. Sciences 48 (2009) 154-164, "Performance evaluation of a hybrid photovoltaic thermal (PV/T) (glass-to-glass) system"

[40] E. A. Chávez Urbiola and Y. Vorobiev / Int. J. of Photoenergy 2013, 704087, 7, "Investigation of Solar Hybrid Electric/Thermal System with Radiation Concentrator and Thermoelectric Generator"

[41] Guiqiang Li et al. / Energies 2017, 10, 20, "Analysis of the Primary Constraint Conditions of an Efficient Photovoltaic-Thermoelectric Hybrid System"

[42] S. Mahmoudinezhad et al. / Energy Conv. and Mng. 164 (2018) 443-45, "Behavior of hybrid concentrated photovoltaic-thermoelectric generator under variable solar radiation"

[43] R. Bjørk, K. K. Nielsen / Energy Conv. and Mgt. 156 (2018) 264-268, "The maximum theoretical performance of unconcentrated solar photovoltaic and thermoelectric generator systems"

[44] BirolKılkış / Solar Energy 200 (2020) 89-107, "Development of a composite PVT panel with PCM embodiment, TEG modules, flat-plate solar collector, and thermally pulsing heat pipes"

[45] S. Mahmoudinezhad et al. / Energy Conversion and Management 184 (2019) 448-455, "Experimental and numerical study on the transient behavior of multi-junction solar cell-thermoelectric generator hybrid system"

[46] Samson Shittu et al. / Renewable and Sustainable Energy Reviews 109 (2019) 24-54, "Advancements in thermoelectric generators for enhanced hybrid photovoltaic system performance"

[47] Jin Zhang, Yimin Xuan / Solar Energy 177 (2019) 293-298, "An integrated design of the photovoltaic-thermoelectric hybrid system"

[48] P. Bamroongkhan et al. / Energy Procedia 158 (2019) 528–533, "Experimental performance study of a solar parabolic dish photovoltaic-thermoelectric generator"

[49] Shuang-Ying Wu et al. / Int. J. of Sustainable Energy, 2018, 37, 6, 533–548, "Performance comparison investigation on solar photovoltaic thermoelectric generation and solar photovoltaic-thermoelectric cooling hybrid systems under different conditions"

[50] A. Lekbir et al. / Int. J. of Green Energy 2019, 16, 5, 371–377, "Higher-efficiency for combined photovoltaic-thermoelectric solar power generation"

[51] F. Souayfane et al. / Energy and Buildings 129 (2016) 396–431, "Phase change materials (PCM) for cooling applications in buildings: A review"

[52] Tao Ma et al. / Renewable and Sustainable Energy Reviews 43 (2015) 1273-1284, "Using phase change materials in photovoltaic systems for thermal regulation and electrical efficiency improvement: A review and outlook"

[53] Pascal Henry Biwole et al. / Energy and Buildings 62 (2013) 59-67, "Phase-change materials to improve solar panel's performance"

[54] Farouk Hachem et al. / Renewable Energy 107 (2017) 567-575, "Improving the performance of photovoltaic cells using pure and combined phase change materials – Experiments and transient energy balance"

[55] Rok Stropnik, Uroš Stritih / Renewable Energy 97 (2016) 671-679, "Increasing the efficiency of PV panel with the use of PCM"